Mutations Affecting the SAND Domain of DEAF1 Cause Intellectual Disability with Severe Speech Impairment and Behavioral Problems

Anneke T. Vulto-van Silfhout,[1,14] Shivakumar Rajamanickam,[2,14] Philip J. Jensik,[2,14] Sarah Vergult,[3] Nina de Rocker,[3] Kathryn J. Newhall,[4] Ramya Raghavan,[2] Sara N. Reardon,[2] Kelsey Jarrett,[2] Tara McIntyre,[2] Joseph Bulinski,[2] Stacy L. Ownby,[2] Jodi I. Huggenvik,[2] G. Stanley McKnight,[4] Gregory M. Rose,[2,5] Xiang Cai,[2] Andy Willaert,[3] Christiane Zweier,[6] Sabine Endele,[6] Joep de Ligt,[1] Bregje W.M. van Bon,[1] Dorien Lugtenberg,[1] Petra F. de Vries,[1] Joris A. Veltman,[1] Hans van Bokhoven,[1,7] Han G. Brunner,[1] Anita Rauch,[8,9,10] Arjan P.M. de Brouwer,[1,7] Gemma L. Carvill,[11] Alexander Hoischen,[1] Heather C. Mefford,[11] Evan E. Eichler,[12,13] Lisenka E.L.M. Vissers,[1] Björn Menten,[3] Michael W. Collard,[2,15] and Bert B.A. de Vries[1,15,*]

Recently, we identified in two individuals with intellectual disability (ID) different de novo mutations in *DEAF1*, which encodes a transcription factor with an important role in embryonic development. To ascertain whether these mutations in *DEAF1* are causative for the ID phenotype, we performed targeted resequencing of *DEAF1* in an additional cohort of over 2,300 individuals with unexplained ID and identified two additional individuals with de novo mutations in this gene. All four individuals had severe ID with severely affected speech development, and three showed severe behavioral problems. *DEAF1* is highly expressed in the CNS, especially during early embryonic development. All four mutations were missense mutations affecting the SAND domain of DEAF1. Altered DEAF1 harboring any of the four amino acid changes showed impaired transcriptional regulation of the *DEAF1* promoter. Moreover, behavioral studies in mice with a conditional knockout of *Deaf1* in the brain showed memory deficits and increased anxiety-like behavior. Our results demonstrate that mutations in *DEAF1* cause ID and behavioral problems, most likely as a result of impaired transcriptional regulation by DEAF1.

Introduction

Intellectual disability (ID) is a highly heterogeneous disorder that is frequently caused by de novo gene mutations.[1–4] Hence, exome sequencing of the individuals involved and their parents (trio approach) is an effective way of identifying the underlying cause. Recently, we and others showed that in 16%–31% of individuals with ID, mutations in genes associated with ID could be identified via trio-based exome sequencing.[1,2,4,5] In an additional ~20% of these individuals, a de novo mutation was identified in a candidate gene that was not previously associated with ID.[1,2,4] For these candidate genes associated with ID, it is often difficult to determine whether the de novo mutation is causative for the ID phenotype. To establish their role in an ID phenotype, it is essential to identify other individuals with both de novo mutations in the same gene and a similar phenotype and/or to perform functional assays to assess the effect of the amino acid change on the respective protein. For one of these candidate genes, DEAF1 transcription factor (*DEAF1* [MIM 602635; RefSeq accession number NM_021008.2]), de novo mutations were identified in two independent studies in two unrelated individuals with severe ID.[2,4]

DEAF1 encodes deformed epidermal autoregulatory factor 1 homolog (DEAF1), a transcription factor that binds to TTCG motifs in DNA.[6] It is involved in the regulation of various genes,[7] including itself, as both a transcriptional activator[8–10] and a repressor.[11,12] DEAF1 comprises multiple structural domains: a SAND (Sp-100, AIRE, NucP41/75, and DEAF1) domain, which is essential for DNA binding (via its KDWK motif) and protein-protein interactions;[11,13,14] a MYND (myeloid translocation protein 8, Nervy, and DEAF1) domain, which is a cysteine-rich module also involved in protein-protein interactions;[15,16] and a nuclear localization signal and a nuclear export signal important for nuclear localization of DEAF1.[6] A region within the nuclear export signal and another in the SAND domain also mediate DEAF1 multimerization, which is required for DNA binding.[15,17] Disruption of *Deaf1* in

[1]Department of Human Genetics, Radboud University Medical Center, 6500 HB Nijmegen, the Netherlands; [2]Department of Physiology and Center for Integrated Research in Cognitive & Neural Sciences, Southern Illinois University School of Medicine, Carbondale, IL 62901, USA; [3]Center for Medical Genetics, Ghent University, Ghent 9000, Belgium; [4]Department of Pharmacology, University of Washington, Seattle, WA 98195, USA; [5]Department of Anatomy, Southern Illinois University School of Medicine, Carbondale, IL 62901, USA; [6]Institute of Human Genetics, Friedrich-Alexander-Universität Erlangen-Nürnberg, 91054 Erlangen, Germany; [7]Department of Cognitive Neurosciences, Radboud University Medical Center, 6500 HB Nijmegen, the Netherlands; [8]Institute of Medical Genetics, University of Zurich, 8603 Schwerzenbach-Zurich, Switzerland; [9]Neuroscience Center Zurich, University of Zurich, 8603 Schwerzenbach-Zurich, Switzerland; [10]Zurich Center of Integrative Human Physiology, University of Zurich, 8603 Schwerzenbach-Zurich, Switzerland; [11]Division of Genetic Medicine, Department of Pediatrics, University of Washington, Seattle, WA 98195, USA; [12]Department of Genome Sciences, University of Washington School of Medicine, Seattle, WA 98195, USA; [13]Howard Hughes Medical Institute, Seattle, WA 98195, USA
[14]These authors contributed equally to this work
[15]These authors contributed equally to this work
*Correspondence: bert.devries@radboudumc.nl
http://dx.doi.org/10.1016/j.ajhg.2014.03.013.

animal models produces neural-tube defects in mice[18] and early embryonic arrest in *Drosophila*.[19] In humans, DEAF1 has previously been associated with major depression and suicide,[20–22] autoimmune disorders,[7] and cancer.[8,23]

Here, we aimed to determine whether de novo mutations affecting the SAND domain of DEAF1 could be the underlying cause of ID in humans by (1) identifying and deeply phenotyping multiple individuals with de novo mutations in *DEAF1*, (2) assessing the effect of the human amino acid substitutions on DEAF1 function, and (3) studying the phenotypic effect of the disruption of *Deaf1* in a mouse model. The results show that mutations affecting the SAND domain of the transcription factor DEAF1 might lead to ID with severely affected expressive speech and behavioral abnormalities.

Subjects and Methods

Identification of Individuals with *DEAF1* Mutations

Targeted resequencing of the coding sequence of *DEAF1* was performed in two cohorts of individuals with unexplained ID. The first cohort of 765 individuals was resequenced after targeted array-based enrichment as described before,[1] whereas the second cohort of 1,561 individuals was assayed with molecular inversion probes (MIPs) as described previously.[24] Both of these cohorts were selected from the in-house collection of the Department of Human Genetics of Radboud University Medical Center (Nijmegen) and consisted of over 5,000 samples from individuals with unexplained ID. Candidate mutations were tested by standard Sanger sequencing approaches on DNA extracted from peripheral blood. For assessing the de novo occurrence of confirmed mutations, DNA from the parents was tested. This study was approved by the institutional review board Commissie Mensgebonden Onderzoek Regio Arnhem-Nijmegen NL36191.091.11. Written informed consent was obtained from all individuals.

Assessment of *DEAF1* Expression

DEAF1 expression was assessed in different human fetal and adult tissues and in mouse brain by quantitative PCR (qPCR). In addition, the expression of the *DEAF1* orthologs *deaf1-a* (zgc:194895) and *deaf1-b* (zgc:171506) in zebrafish was assessed by in situ hybridization and qPCR at different time points.

Assessment of Altered DEAF1

Plasmids and Site-Directed Mutagenesis

DEAF1 mammalian expression plasmids in pcDNA3 and fused in-frame to a carboxy-terminal FLAG epitope tag were derived from the human *DEAF1* cDNA (GenBank accession number AF049459) and have been previously described.[11,15] Site-directed mutagenesis to introduce the p.Arg224Trp (c.670C>T), p.Ile228Ser (c.683T>G), p.Gln264Pro (c.791A>C), and p.Arg254Ser (c.762A>C) amino acid substitutions into the DEAF1 expression plasmids were generated by PCR using primers containing the indicated human amino acid substitutions. Primers also contained specific DEAF1 native restriction endonuclease sites to facilitate subcloning. Digested PCR fragments were used to replace the corresponding regions of wild-type (WT) DEAF1. The reporter plasmid pDEAF1pro-luciferase is similar to the previously described pNUDRproCAT6[11] and was constructed by subcloning of the 1,150 bp region 5′ to the ATG start codon of the human *DEAF1* promoter into the pGL3 basic firefly luciferase reporter plasmid (Promega). The mouse *Eif4g3* promoter region from −609 to +58 (relative to the transcription start site) was amplified from mouse genomic DNA by PCR (primers are in Table S1, available online), and the product was subcloned into the NheI and HindIII sites of the pGL3 basic plasmid. All plasmid constructs were confirmed by DNA sequencing by a Beckman Coulter CEQ 8000 Genetic Analysis System.

Transcription Assay

Human embryonic kidney 293T (HEK293T) cells were plated in 24-well plates (90,000 cells per well) and transfected with 125 ng pcDNA3 (control) or DEAF1 (expressing WT or altered DEAF1) expression plasmids, along with 375 ng pDEAF1pro-luciferase or pEif4g3pro-luciferase and 1.25 ng Rous sarcoma virus (RSV)-*Renilla* (for normalization), via the calcium phosphate technique. Media were replaced 18 hr later, and luciferase assays were performed 24 hr later with the Dual-Luciferase Reporter Assay System (Promega) according to the manufacturer's protocol.

Purification of Recombinant FLAG-Tagged Proteins

HEK293T cells were transfected with 10 μg of expression plasmids for WT or altered FLAG-tagged DEAF1. Cell lysates were prepared in lysis buffer P (150 mM NaCl, 50 mM Tris, pH 7.5, 1 mM EDTA, 1% Triton X-100, 1 mM DTT, 1 mM NaF, and Complete Protease Inhibitor Cocktail [Roche]) on ice, and cell debris were removed by centrifugation. Lysates were incubated with anti-FLAG beads overnight at 4°C. Proteins bound to the beads were washed four times with lysis buffer P and once with Tris-buffered saline (TBS: 50 mM Tris, pH 7.4, and 150 mM NaCl) before elution with 200 ng/ml FLAG in TBS for 30 min on ice and then the addition of glycerol to 50%. Protein concentrations were calculated by Coomassie blue staining and comparison to BSA standards after SDS-PAGE (Figure S1). Band intensities were quantified on a Li-Cor Odyssey CLx.

GST Pull-downs to Examine DEAF1 and XRCC6 Interactions

Glutathione S-transferase (GST) and GST-XRCC6 fusion proteins were purified as previously described.[14] FLAG-tagged WT and altered DEAF1 were purified from transfected HEK293T cells as previously described (see above and Jensik et al.[14]). Five hundred nanograms of GST or GST-XRCC6 attached to glutathione beads was incubated with 100 ng of purified WT or altered FLAG-tagged DEAF1 in interaction buffer (50 mM NaCl, 20 mM Tris, pH 7.9, 0.1% Nonidet P-40, 10% glycerol, 1 mM dithiothreitol, and 0.25% BSA) overnight at 4°C. Beads were then washed six times with interaction buffer, and proteins were eluted from beads with Laemmli sample buffer. Eluted samples and similar amounts of purified FLAG-tagged DEAF1 used in the GST pull-down (inputs) were separated on SDS-PAGE gels and transferred to polyvinylidene fluoride membrane. Immunoblot analysis was then performed with an anti-DEAF1 antibody.[6]

Electrophoretic Mobility Shift Assays

For electrophoretic mobility shift assays (EMSAs), we used full-length recombinant DEAF1 isolated from HEK293 cells (Figure S1) and two DNA ligands for DEAF1—the first consisted of two TTCG motifs spaced by 11 nucleotides and was based on a sequence found in the human *DEAF1* promoter,[11,12] and the second had two TTCG motifs spaced by 6 nucleotides. This latter sequence was a high-affinity ligand and was based on the preferred binding motif of DEAF1 (data not shown). Fluorescently labeled double-stranded DNA (dsDNA) probes with 11 or 6 bp spacing of CG dinucleotides were generated by hybridization of oligonucleotides N52-69F and N52-69R or S6conF and S6conR, respectively

(Table S1). Oligonucleotides were labeled at their 5′ ends with IRDye800 (N52-69) or IRDye700 (S6con) and purified by high-performance liquid chromatography (Integrated DNA Technologies). WT and altered FLAG-tagged DEAF1 from HEK293T cells (850 fmol) were incubated with 500 fmol of dsDNA probe and 1 μg of poly(dA-dT) (nonspecific competitor) in a 20 μl reaction containing 70 mM KCl, 35 mM Tris, pH 7.5, 0.7 mM DTT, 1 mM $MnSO_4$, 2% (v/v) glycerol, and 100 U of lambda protein phosphatase (New England Biolabs) for 20 min at 25°C. Protein-DNA complexes were separated as previously described,[11] and band intensities were quantified on a Li-Cor Odyssey CLx.

Subcellular Localization

HEK293T cells on 35 mm dishes were cotransfected with 500 ng of expression plasmids for WT or altered FLAG-tagged DEAF1 and 500 ng pcDNA3 or hemagglutinin (HA)-tagged p.Lys304Thr DEAF1 expression plasmids via the calcium phosphate technique. Twenty-four hours later, cells were fixed in paraformaldehyde, permeabilized in methanol, and incubated with rabbit anti-HA (1:1,000 Santa Cruz) and mouse anti-FLAG (1:1,000 Sigma Aldrich) antibodies followed by Alexafluor-488-conjugated goat anti-rabbit IgG and Cy3-conjugated donkey anti-mouse IgG. Cells were visualized with an Olympus BW50 fluorescence microscope with a 60× water objective.

Generation of Mouse Knockout Models for *Deaf1*

Mice with a targeted disruption of exons 2–5 of *Deaf1* (*Deaf1*$^{+/-}$ mice) were produced (Figure S3) and then backcrossed onto a C57BL/6 background for seven generations before F1 crosses were performed. In addition, a conditional knockout of *Deaf1* in mouse brain was produced with mice with loxP sites flanking exons 2–5 of *Deaf1* ("floxed," *Deaf1*$^{+/fl}$ mice) (Figure S3). These were bred to congenic status onto a C57BL/6 background and were then bred to mice transgenic for nestin-*cre* (*Nes-cre*); these latter mice express Cre recombinase in neuronal and glial precursors by embryonic day 11.[25] Subsequent breeding produced mice with the genotype *Deaf1*$^{fl/fl;Nes\text{-}cre}$, resulting in neuronal homozygous knockout (NKO) of *Deaf1* (these mice are hereafter referred to as NKO mice). Mice with a single conditional *Deaf1* allele and positive for *Nes-cre* have the genotype *Deaf1*$^{+/fl;Nes\text{-}cre}$. Mice with any combination of WT or floxed *Deaf1* alleles but lacking *Nes-cre* are referred to as control mice. Detailed protocols and supporting data for these procedures are provided in the Supplemental Data.

Phenotyping of Mice with Conditional Targeting of *Deaf1*

Mice were tested for anxiety with the elevated plus maze (EPM) and the open-field test. The EPM tests for an animal's conflict between exploration and fear of open and/or elevated places. The EPM consists of two opposed closed arms (44 × 6 cm) with raised walls (18 cm high) crossing with two open arms (44 × 6 cm) without walls. A central platform (6 × 6 cm) links the open and closed arms. The apparatus is elevated to a height of 55 cm from the floor. A mouse is placed in the central platform and allowed to explore the maze for 5 min, and movements are recorded with a digital camera and computer and analyzed with the ANY-maze software program (San Diego Instruments) for time spent and distance traveled. Open-field exploration also tests for unconditioned behavior and is designed to evaluate the total amount and rate of movement and the type of spontaneous activity and to provide a partially specific measure of anxiety-related behavior. The equipment consists of an open box (58 × 58 cm), and the animal is placed in the central arena, from which it is free to explore the box for 5 min. Mice prefer to stay near the walls of the box and avoid the center zone, which induces the conflict. Reduced time spent and distance traveled in the center zone is indicative of increased anxiety-like behavior in mice. Paths were recorded and analyzed with ANY-maze software.

The EPM and the open-field test were performed from 10 a.m. to 3 p.m. with constant illumination (50 lux). Between animals, testing surfaces were wiped with 70% ethanol followed by distilled water and then dried completely.

Learning and memory were tested with the Morris water maze and fear-conditioning tests. A white, circular tank 1 m in diameter and 30 cm deep was filled with 22°C –24°C water to a depth of 20 cm. Mice were tested in the water maze for 9 days. The animals were first trained for three trials per day for 3 days with a visible escape platform raised 1 cm above the water line. The interval between each trial was approximately 1 hr. On the fourth training day, the platform was moved to the opposite quadrant of the pool and submerged 1 cm below the surface of the water. The mice were given 5 days of hidden platform training, as well as three trials per day with a 1 hr intertrial interval. A 1 minute probe trial, with the platform removed from the pool, was given 7 days after the last hidden-platform trial. For both visible- and hidden-platform training, every trial began from a different starting position, and the mouse was placed in a beaker facing the wall of the tank. If the mouse did not locate the platform within the allotted time, it was placed on the platform by the experimenter. Mice were left on the platform for 30 s at the end of each trial before being removed from the tank with a large metal spoon and placed under a heat lamp for 5–10 min before being returned to their home cages for 1 hour before the next trial. Swim times and distances during training, as well as probe-trial parameters, were collected with ANY-maze software. Statistical analysis was performed with a two-way repeated-measures ANOVA (genotype × trials) followed by a Bonferroni posttest to analyze escape latencies in visible- and hidden-platform testing. A two-way ANOVA (genotype × quadrants) followed by a Bonferroni posttest was used to analyze the time spent in each quadrant during the first trial of hidden-platform testing and for the probe trial. For fear conditioning, mice were placed on the first day in a test chamber (30.5 cm length × 24.1 cm width × 21.0 cm height, Standard Modular Test Chamber ENV-008, Med Associates) for a conditioning session of 4 min 90 s of habituation, a 2 s foot shock (0.5 mA), 90 s of no stimuli, another foot shock, and a final 60 s of no stimuli. Twenty-four hours after the conditioning session, mice were placed in the test chamber again for 5 min for testing contextual fear conditioning. The percentage of time spent freezing was quantified by video image analysis (Freeze Frame, Coulbourne Instruments) and ANOVA. After the fear-conditioning test, foot-shock-sensitivity testing was performed as outlined in Figure S9.

Depression-related behavior was tested by sucrose preference (a test for anhedonia) and the forced swim test, whereas balance and mobility were tested by an accelerating-rotarod test. Detailed methodology of these three tests is provided in Figure S7.

Results

Individuals with De Novo Mutations in *DEAF1*

Upon the identification of two separate de novo mutations in *DEAF1* by trio-based exome sequencing in two independent cohorts encompassing 10 and 51 individuals with

Table 1. Molecular and Clinical Details of Individuals with *DEAF1* Mutations

Molecular and Clinical Details	Individual 1[4]	Individual 2[2]	Individual 3	Individual 4
Gender	male	female	male	female
Age at last visit	9 years	7 years	10 years	10 years
Parental age	mother, 32 years father, 35 years	mother, 31 years father, 32 years	mother, 29 years father, 30 years	mother, 40 years father, 48 years
Mutations				
Amino acid change[a]	p.Ile228Ser	p.Gln264Pro	p.Arg224Trp	p.Arg254Ser
cDNA change[b]	c.683T>G	c.791A>C	c.670C>T	c.762A>C
Chromosome position[c]	chr11: 686,979	chr11: 686,871	chr11: 686,992	chr11: 686,900
PhyloP[26]	4.4	2.5	3.4	−0.4[d]
SNPs&GO[27]	disease related	disease related	disease related	disease related
MutPred[28]	0.825	0.659	0.551	0.539
PolyPhen-2[29]	0.984	0.972	0.996	0.999
Growth				
Birth weight (g)	−2 SDs	−0.5 SD	+0.7 SD	NR
Height (cm)	−1.3 SDs	−0.6 SD	−0.4 SD	−1.7 SDs
Weight (kg)	+0.5 SD	−1.5 SDs	−0.8 SD	0 SD
Head circumference (cm)	−0.6 SD	+0.1 SD	−1 SD	+0.3 SD
Development				
Motor delay	mild	mild	mild	mild
Expressive speech[e]	absent	ten single words	absent	disappeared at 18 months
Intellectual disability	severe	moderate	severe	severe
Regression	−	−	+	+
Neurological				
Contact	poor eye contact	good	poor eye contact	poor eye contact
Hypotonia	−	+	−	−
Behavioral problems	+	−	+	+
Autism	+	−	+	+
Mood swings	+	−	+	+
Fascinations	+	NR	NR	+
High pain threshold	+	in childhood	+	+
Sleeping problems	−	−	+	+
Abnormal walking pattern	+	+	+	+
Abnormal brain MRI	NR	−	−	+
Facial				
Thin and/or fair hair	+	+	−	+
Straight eyebrows	+	+	+	+
Full nasal tip	+	+	+	+
Cupid's bow in upper lip	−	+	+	+
Full lower lip	+	+	−	+

(*Continued on next page*)

Table 1. *Continued*

Molecular and Clinical Details	Individual 1[4]	Individual 2[2]	Individual 3	Individual 4
Prominent chin	+	−	+	+
Other	upslant, epicanthic folds	frontal bossing, high palate	brachycephaly, widow's peak, flat face	NR
Extremities				
Fetal finger pads	+	−	+	−
Skin syndactyly in toes 2 and 3	+	+	+	−
Hyperlaxity	+	+	−	−
Other				
Recurrent infections	in childhood	+	+	in childhood
Sacral dimple	−	+	+	−
Other clinical features	scrotal raphe, flat feet	sandal gap	20–40 dB hearing loss, clinodactyly in toes 3 and 4, dry skin	clinodactyly in toes 4 and 5
Other detected gene mutations	NR	*DOCK9* c.1604C>T (p.Ala535Val) and *CDK18* c.118C>T (p.Arg40Trp)	*SCN2A* c.1570C>T (p.Arg524*)	NR

The following abbreviation is used: NR, not reported.
[a]RefSeq NP_066288.
[b]RefSeq NM_021008.2.
[c]UCSC Genome Browser hg19.
[d]This base is the third base of a codon.
[e]Speech comprehension was significantly better in all four individuals.

severe ID,[2,4] we performed targeted resequencing of *DEAF1* in an additional cohort of over 2,300 individuals with ID. Here, we identified two additional individuals with a de novo mutation in *DEAF1*, resulting in a total of four individuals with de novo mutations in this gene: c.683T>G (p.Ile228Ser), c.791A>C (p.Gln264Pro), c.670C>T (p.Arg224Trp), and c.762A>C (p.Arg254Ser) (Table 1, Figures 1A and 1B). All children (age range 7–10 years) showed moderate to severe ID with severely affected expressive speech and only mild motor delay (Table 1). All had a happy predisposition, but three had severe behavioral problems consisting of autistic, hyperactive, compulsive, and aggressive behavior with striking mood swings. Other frequently observed abnormalities were recurrent infections, a high pain threshold, and an abnormal walking pattern. All had normal body measurements, only mild dysmorphism (Figure 1A), and no further congenital anomalies.

DEAF1 mRNA Expression

qPCR analysis of *DEAF1* mRNA in various human fetal and adult tissues showed that *DEAF1* was expressed more than 30 times higher in fetal and adult brain than in the duodenum (Figure S2C). In addition, qPCR analysis of *Deaf1* mRNA expression in the brain of adult mice showed that *Deaf1* was expressed 5–20× higher in various brain regions than in the liver (Figure S5). Therefore, we used in situ hybridization at various embryonic stages of zebrafish to study the expression pattern of *deaf1-a* and *deaf1-b*, which share 53% and 36% homology, respectively, with human *DEAF1*. This showed the highest expression in the brain and spinal cord of both orthologs (Figure S2A). Expression quantification by qPCR showed that *deaf1-a* was transiently expressed about three times higher at 24 days post-fertilization (dpf) than at 14 dpf (Figure S2B), whereas expression of *deaf1-b* was very low to absent at all embryonic stages (data not shown).

Functional Consequences of *DEAF1* Mutations

All four de novo mutations found in these individuals were missense mutations affecting evolutionary conserved amino acids within the SAND domain (Figures 1C and 1D) and were predicted by SNPs&GO,[27] MutPred,[28] and PolyPhen-2[29] to be detrimental to protein function (Table 1). None of these mutations were present in dbSNP v.139, the NHLBI Exome Sequencing Project Exome Variant Server, or our in-house database containing exome data of over 2,000 individuals. In silico modeling by Project HOPE (Have Your Protein Explained)[30] with the mouse putative nuclear protein ortholog (SP110 [Protein Data Bank ID 1UFN], which shares 40% homology with the human DEAF1 SAND domain) as a template predicted that all four amino acid substitutions might affect SAND domain function either by directly interfering with the DNA-interaction surface or by disturbing the core structure of this domain (Figure 2A). Therefore, we compared the

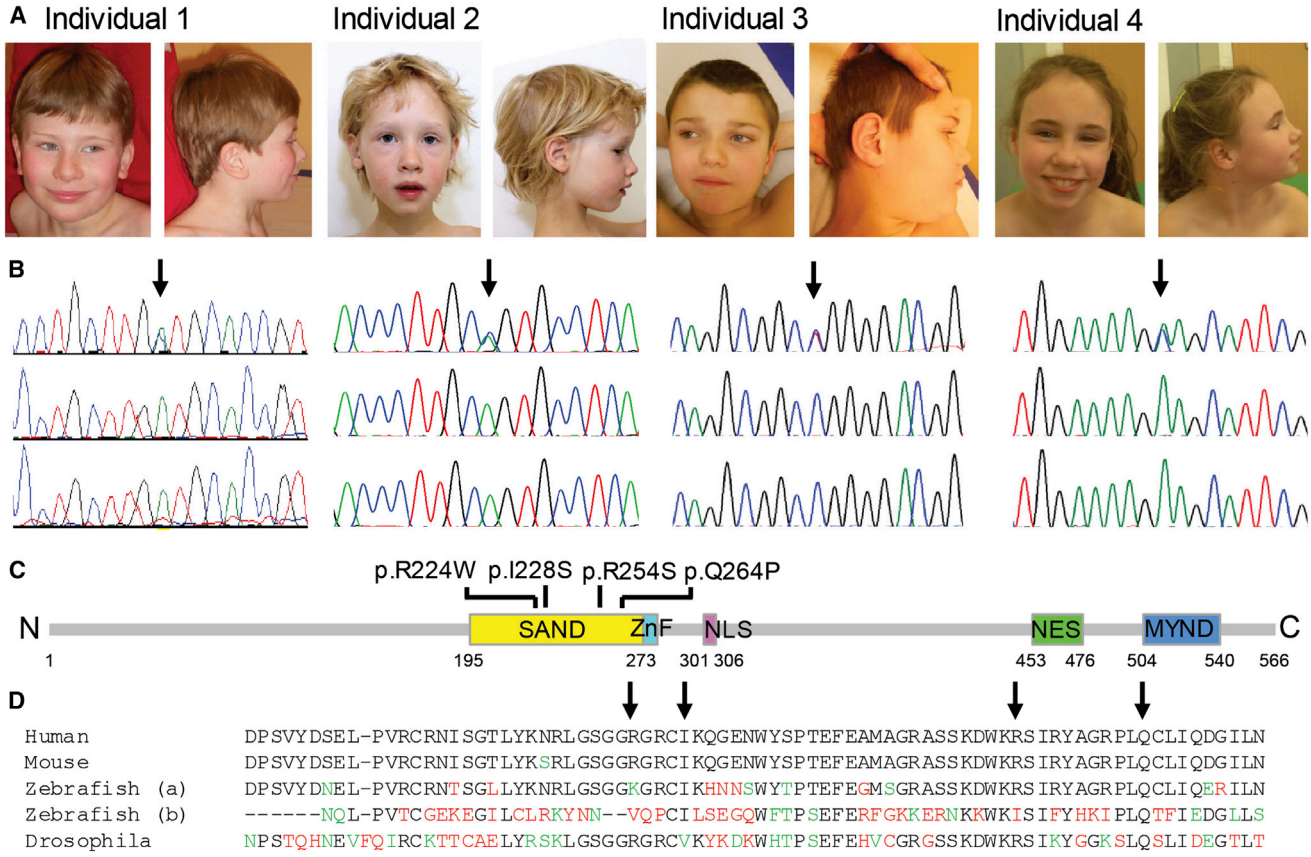

Figure 1. Individuals with *DEAF1* Mutations

(A) Frontal and lateral photographs of individuals with de novo mutations in *DEAF1*. Only mild facial dysmorphisms were observed.

(B) Sanger sequencing chromatograms showing the *DEAF1* mutations in the proband (top panel), but not in the parents (bottom panels).

(C) Schematic overview of DEAF1, including the known domains (SAND domain, zinc-finger homology [ZnF] domain, nuclear localization signal [NLS], nuclear export signal [NES], and MYND domain). The positions of the four identified missense substitutions (p.Arg224Trp [p. R224W], p.Ile228Ser [p.I228S], p.Arg254Ser [p.R254S], and p.Gln264Pro [p.Q264P]) in the SAND domain are depicted.

(D) Multispecies alignment of the SAND domain in eukaryotes. Amino acid residues with substitutions are indicated by arrows. Amino acids with similar properties are marked in green, and dissimilar amino acids are marked in red. Zebrafish "a" is zgc:194895, and zebrafish "b" is zgc:171506.

functional activities of WT DEAF1 and of altered DEAF1 harboring either of the four identified amino acid substitutions along with two previously described alterations affecting the SAND domain.[11]

It was previously shown that DEAF1 represses its own *DEAF1* promoter and that amino acid substitutions affecting the SAND domain can eliminate DNA binding and promoter repression.[11,12] In a reporter assay with the human *DEAF1* transcriptional promoter fused to a luciferase reporter gene, overexpression of DEAF1 containing any of the four amino acid substitutions resulted in a loss of the ability to repress the *DEAF1* promoter (Figure 2B). A similar loss of *DEAF1*-promoter repression was observed for the previously characterized combined p.Lys250Ala and p.Lys253Ala substitutions, localized within the essential positively charged surface of the KDWK motif, whereas the randomly selected p.Arg226Ala change, located between the amino acid substitutions identified in this study (p.Arg224Trp and p.Ile228Ser), had no effect on transcriptional repression,[11] indicating that the amino acid substitutions identified in this study are specifically deleterious.

DEAF1 has also been shown to function as a transcriptional activator of eukaryotic translation initiation factor 4 gamma, 3 (*Eif4g3* [RefSeq accession number NM_172703]).[8,10] Relative to basal transcription, WT DEAF1 produced about a 2-fold activation of the mouse *Eif4g3* reporter construct, whereas the amino acid substitution identified in this study (p.Arg224Trp) showed no activation (Figure 2C). Both amino acid substitutions p.Ile228Ser and p.Gln264Pro showed not only loss of transcriptional activation but also an approximate 10-fold suppression of transcription relative to basal expression levels, whereas the amino acid substitution identified in this study (p.Arg254Ser) and the randomly selected substitution p.Arg226Ala continued to activate *Eif4g3* reporter expression.

Because the SAND domain mediates DEAF1 DNA binding, we performed EMSAs to examine whether impaired DNA binding could underlie the impaired transcriptional

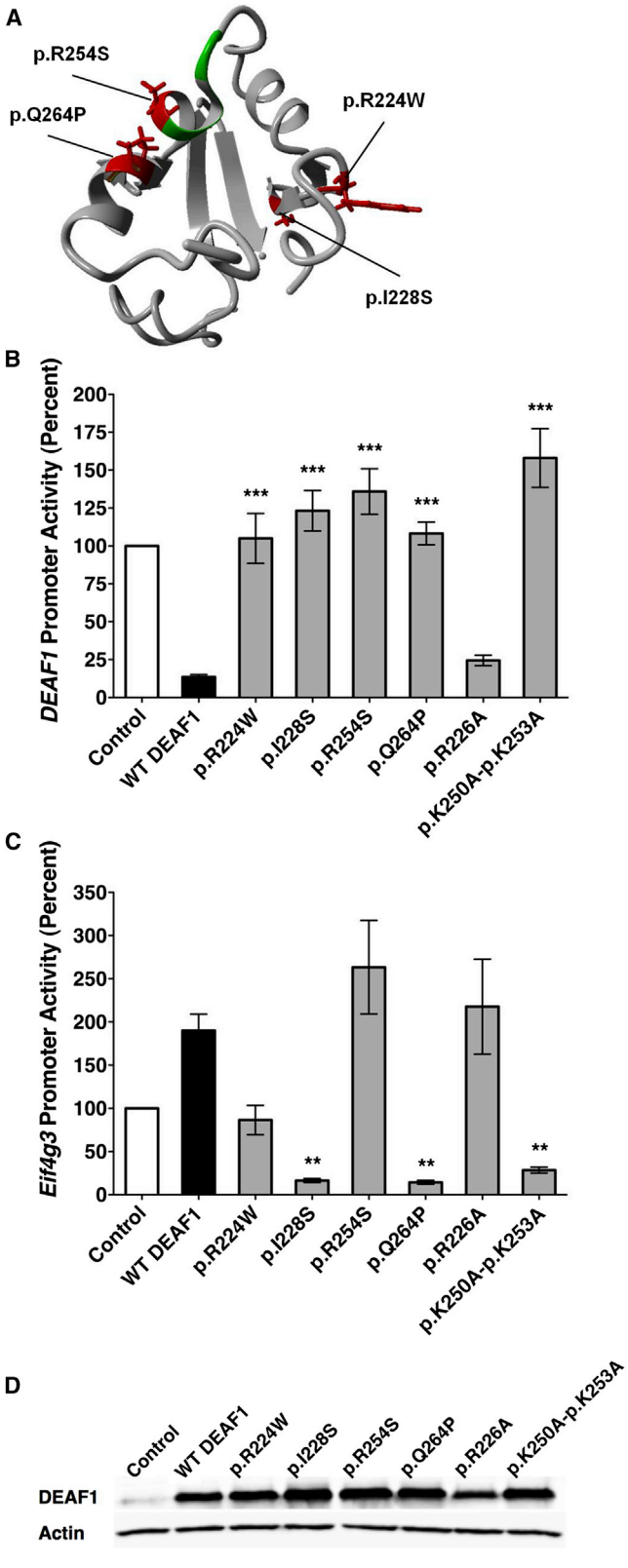

Figure 2. *DEAF1* Mutations Alter Transcriptional Regulation

(A) This 3D model of the SAND domain is based on the homologous structure from the mouse putative nuclear protein homolog (SP110); the four amino acid substitutions are in red, and the essential KDWK motif is in green.

(B) *DEAF1* promoter activity after transfection with either WT or altered FLAG-tagged DEAF1. Similar to the previously characterized combined p.Lys250Ala and p.Lys253Ala substitutions, the substitutions identified in this study (p.Arg224Trp [p.R224W], p.Ile228Ser [p.I228S], p.Arg254Ser [p.R254S], and p.Gln264Pro [p.Q264P]) were unable to repress *DEAF1* promoter activity. The p.Arg226Ala (p.R226A) substitution had no effect on transcriptional repression. Each bar represents the mean ± SEM of the normalized luciferase activity of three independent experiments when the activity of pcDNA3 (*DEAF1* promoter alone) was set to 100%. One-way ANOVA with both Dunnett's multiple comparison and selected Bonferroni posttest of WT DEAF1 versus each mutant, ***$p < 0.001$.

(C) Promoter activity of mouse *Eif4g3* after transfection with either WT or altered FLAG-tagged DEAF1. Relative to basal transcription, WT DEAF1 and p.Arg254Ser altered DEAF1 produced about a 2-fold activation of the reporter construct, whereas the p.Arg224Trp altered DEAF1 showed no activation. Both the p.Ile228Ser and the p.Gln264Pro proteins showed not only a loss of transcriptional activation but also an approximately 10-fold suppression of transcription relative to basal expression levels. The results are from three independent experiments and analyzed as in (B). **$p < 0.01$.

(D) Immunoblot analysis for transfected amounts of FLAG-tagged DEAF1 in HEK293T cells. Equal quantities of transfected cell lysates were assayed for WT and altered FLAG-tagged DEAF1 with the use of anti-DEAF1 antibody (anti-actin antibody was used as a loading control). DEAF1 amounts were similar in the transfected cell lysates.

regulation. For DEAF1, we utilized two DNA ligands, one based on a sequence found in the human *DEAF1* promoter[11,12] and one based on the preferred binding motif of DEAF1 (data not shown; Table S1). Recombinant DEAF1 containing the amino acid substitutions identified in this study (p.Arg224Trp, p.Ile228Ser, and p.Gln264Pro) showed a complete loss of DNA binding to both DNA ligands, whereas p.Arg254Ser altered DEAF1 displayed a 9-fold reduction in binding of the DNA ligand with 11 bp CG-spacing and a 53-fold reduction in the DNA ligand with 6 bp CG spacing (Figure 3A). Thus, all four of the ID-associated mutations produce proteins with loss of or highly reduced DNA binding.

The SAND domain of DEAF1 also mediates DEAF1 multimerization, which is required for DNA binding.[15] We have previously demonstrated that DEAF1-DEAF1 interactions can be monitored by immunofluorescence and a relocalization of a cytoplasmically localized p.Lys304Thr altered DEAF1 to the nucleus.[15] p.Arg224Trp, p.Ile228Ser, p.Arg254Ser, and p.Gln264Pro altered DEAF1 showed normal localization to the nucleus, and they were all able to relocalize the p.Lys304Thr altered DEAF1 from the cytoplasm to the nucleus (Figure 3C).

The SAND domain of DEAF1 also mediates interaction with X-ray repair cross-complementing protein 6 (XRCC6, also called Ku70 [RefSeq NP_001275905]), which is a subunit of the DNA-dependent protein kinase complex.[14] Using GST-pull-down assays, we showed that the interaction with XRCC6 was greatly reduced for both amino acid substitutions p.Ile228Ser and p.Gln264Pro and mildly reduced for substitution p.Arg224Trp, but XRCC6 interaction with substitution p.Arg254Ser was retained (Figure 3B), indicating that for these substitutions, SAND domain function seems further compromised.

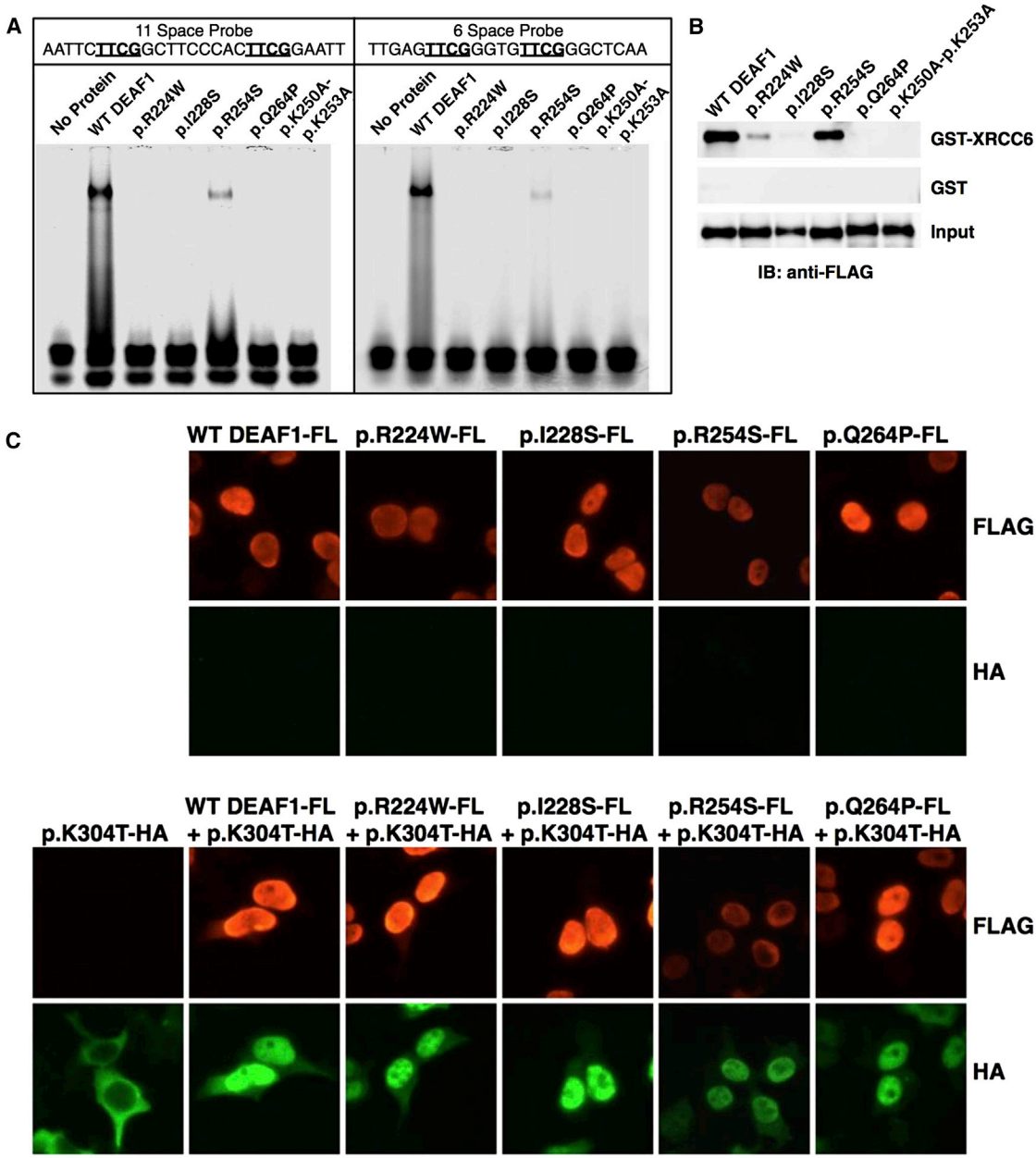

Figure 3. *DEAF1* Mutations Alter DNA and Protein Interactions

(A) EMSA of WT and altered FLAG-tagged DEAF1 recombinant proteins isolated from HEK293T cells. Fluorescently labeled DNA ligands with a spacing of 11 or 6 nucleotides between the CG dinucleotides were examined. The p.Arg224Trp (p.R224W), p.Ile228Ser (p.I228S), and p.Gln264Pro (p.Q264P) proteins lacked DNA binding, whereas the p.Arg254Ser (p.R254S) protein showed less binding than WT DEAF1.

(B) XRCC6 interaction with recombinant FLAG-tagged DEAF1 was assessed in GST pull-downs. GST-XRCC6 could pull down WT DEAF1 and the p.Arg254Ser protein. The p.Arg224Trp protein had reduced interaction, and the p.Gln264Pro and p.Ile228Ser proteins had no interaction. The GST-only control did not pull down DEAF1. Recombinant proteins were detected with anti-FLAG antibodies.

(C) DEAF1-DEAF1 interaction was assessed in an immunofluorescence assay. HEK293T cells were transfected with expression plasmids for WT or altered FLAG-tagged DEAF1 by themselves or in combination with an expression plasmid for the p.Lys304Thr (p.K304T) DEAF1 with an HA epitope tag and were then assayed for location by immunofluorescence with anti-FLAG or anti-HA antibodies. WT and altered FLAG-tagged DEAF1localized to the nucleus. The p.Lys304Thr-HA protein localized to the cytoplasm but relocalized to the nucleus in the presence of WT or altered DEAF1.

Behavior Phenotyping of Mice with Conditional Targeting of *Deaf1*

Mice with a targeted disruption of exons 2–5 of *Deaf1* (*Deaf1*$^{+/-}$ mice) were produced (Figures S3 and S4). On a C57BL/6 background, *Deaf1*$^{-/-}$ neonates died 100% of the time and *Deaf1*$^{+/-}$ mice survived in a 2:1 ratio relative to WT mice (Tables S2–S4), and only 3% of *Deaf1*$^{-/-}$ mice survived on a BALB/c background (Table S5), which precluded behavioral studies. Therefore, we created a conditional knockout model of *Deaf1* in mouse brain by

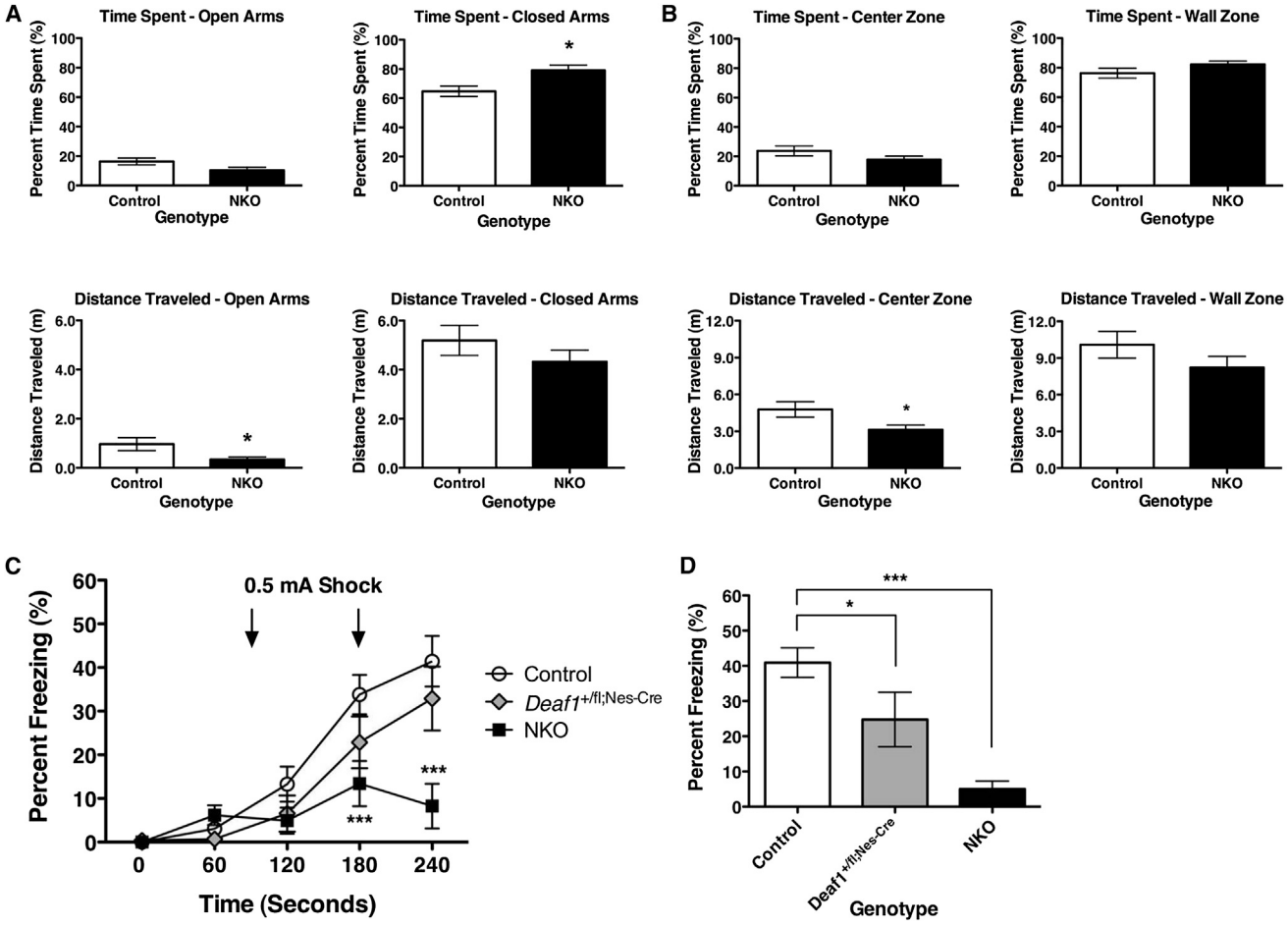

Figure 4. Behavioral Phenotyping of Mice with Conditional Knockout of *Deaf1* in the Brain

(A) Anxiety testing using the EPM. Bars represent the mean ± SEM of the time spent or distance traveled in open and closed arms (control mice, n = 12; NKO mice, n = 12). NKO mice spent significantly more time in the closed arm and traveled significantly less distance in the open arm. Unpaired two-tailed t test, *$p < 0.05$.

(B) Anxiety testing using the open-field test. Bars represent the mean ± SEM of the time spent or distance traveled in the center or wall zones (control mice, n = 12; NKO mice, n = 12). NKO mice displayed significantly reduced distance traveled in the center zone. Unpaired two-tailed t test, *$p < 0.05$.

(C) Percentage of time freezing in response to foot shock. Training on day 1 is shown, and arrows indicate the time of a 0.5 mA shock (control mice, n = 18; $Deaf1^{+/fl;Nes\text{-}cre}$ mice, n = 10; NKO mice, n = 14). Bars represent the mean ± SEM. NKO mice displayed significantly reduced freezing at 180 and 240 s. Two-way repeated-measures ANOVA with Bonferroni posttest between control and NKO mice, ***$p < 0.001$.

(D) Percentage of time freezing in contextual fear conditioning. Context testing 24 hr after training is shown (control mice, n = 18; $Deaf1^{+/fl;Nes\text{-}cre}$ mice, n = 10; NKO mice, n = 14). Bars represent the average of 5 min ± SEM. NKO and $Deaf1^{+/fl;Nes\text{-}cre}$ mice displayed significantly reduced freezing. One-way ANOVA with Bonferroni posttest, *$p < 0.05$, ***$p < 0.001$.

breeding mice with loxP sites flanking exons 2–5 of *Deaf1* ($Deaf1^{+/fl}$) to mice transgenic for *Nes-cre*. NKO mice survived to adulthood at levels similar to those of WT mice, and various brain regions showed 11- to 49-fold reductions of the WT *Deaf1* mRNA transcript (Figure S5).

Adult male mice (median age 4 months) consisting of NKO, $Deaf1^{+/fl;Nes\text{-}cre}$, and control genotypes were sequentially tested with two anxiety tests (the EPM and the open-field test) followed by two tests for depression-related behavior (the sucrose-preference test, which tests for anhedonia, and the forced-swim test). In addition, a second group of adult male mice (median age 7 months) was tested for changes in balance and mobility with an accelerating-rotarod test. In anxiety tests, NKO mice spent statistically significantly more time in the closed arms (NKO mice = 79.0% ± 3.7% versus control mice = 64.7% ± 3.6%, $p < 0.05$) and showed less distance traveled on the open arms of the EPM than did control mice (NKO mice = 0.34 ± 0.10 m versus control mice = 0.97 ± 0.26 m, $p < 0.05$; Figure 4A). NKO mice also displayed less distance traveled in the center zone of the open field than did controls (NKO mice = 3.12 ± 0.38 m versus control mice = 4.77 ± 0.63 m, $p < 0.05$; Figure 4B). Distance traveled in the closed arms of the EPM and the wall zone of the open field was similar between the two genotypes, indicating that the NKO mice did not have mobility deficiencies. Relative to control mice, conditional heterozygous mice ($Deaf1^{+/fl;Nes\text{-}cre}$) did not display any behavior

differences in the anxiety tests (Figure S6). No differences were observed between NKO and control mice for depression-like behavior in the sucrose-preference and forced-swim tests (Figures S7A and S7B) or for rotarod performance (Figure S7C).

Learning and Memory in Mice with Conditional Knockout of *Deaf1*

A group of adult male mice (median age 7 months) was evaluated for changes in learning and memory with the Morris water maze and fear-conditioning testing. All three genotypes showed similar learning curves when they tried to find a visible platform in the Morris water maze (Figure S8A). When mice were retested 48 hr later, NKO mice were significantly faster than control mice at finding a hidden (submerged) platform that had been moved to the opposite quadrant (NKO mice = 42.3 ± 9.3 s versus control mice = 80.3 ± 6.7 s, $p < 0.001$), but only on the first trial with the hidden platform (Figures S8B and S8C). Thereafter, learning curves for the hidden platform were similar among the three genotypes (Figure S8B). When mice were tested with a probe trial 7 days later, no difference in long-term memory was observed (Figure S8D).

Mice were then tested in a contextual fear-conditioning task, wherein the mice were placed into a novel environment and given an electrical foot shock to induce fear memory, as demonstrated by behavioral freezing. NKO mice showed reduced freezing behavior in response to a foot shock (at 240 s, NKO mice = 8.2% ± 5.1% versus control mice = 41.4% ± 5.8%, $p < 0.001$; Figure 4C), and both NKO mice and conditional heterozygous *Deaf1*$^{+/fl;Nes\text{-}cre}$ mice displayed significantly reduced contextual fear memory 24 hr later (NKO mice = 5.0% ± 2.3% and *Deaf1*$^{+/fl;Nes\text{-}cre}$ mice = 24.6% ± 7.7% versus control mice = 40.9% ± 4.2%; Figure 4D). Given that individuals with de novo mutations in *DEAF1* showed increased pain tolerance, a potential explanation for the response in fear conditioning might be a reduced ability to feel the foot shock. However, relative to controls, NKO mice did not display diminished responses to increasing levels of foot shock (Figure S9).

Discussion

Novel sequencing techniques have identified de novo mutations in candidate genes for genetically heterogeneous disorders such as ID. Correlating the clinical consequence of such mutations in these candidate genes is, however, challenging and relies on the identification of additional individuals with mutations affecting the same gene and an overlapping phenotype and functional assays. Here, we describe de novo missense mutations affecting the SAND domain of DEAF1 in four individuals with ID, severe speech impairment, and behavioral problems. We showed that all four of the amino acid substitutions impaired the normal function of DEAF1 in transcriptional regulation of the *DEAF1* promoter and produced loss or greatly reduced binding of DNA ligands. Furthermore, we observed that *DEAF1* was highly expressed in the CNS and that neuronal knockout of *Deaf1* in mice resulted in increased anxiety and deficits in learning and memory. In this way, we have provided further evidence of a causal role for de novo mutations affecting the SAND domain of DEAF1 in the phenotype observed in these individuals.

The phenotype of the individuals with *DEAF1* mutations consisted of moderate to severe ID, disproportionally severely affected expressive speech (but significantly better speech comprehension and motor development), and behavioral problems. Two of the four subjects were identified in preselected cohorts of individuals with moderate to severe ID.[2,4] The other two subjects, however, were identified in a cohort of over 2,300 individuals with unexplained ID (an unselected cohort with the full phenotypic spectrum of individuals with ID), indicating that the ascertainment of these latter individuals was not subjected to selection bias. Because large-scale resequencing efforts have only focused on high-quality variant calls, potentially leaving some true mutations undetected, the true incidence of *DEAF1* mutations affecting the SAND domain of DEAF1 in an unbiased cohort of individuals with ID remains to be determined.

Angelman syndrome (MIM 105830) was considered in the differential diagnosis for all four individuals on the basis of their severely impaired speech development, happy predisposition, fascination with water, and coordination problems, but a diagnostic methylation study of the 15q11–q13 region and/or mutation analysis of *UBE3A* (MIM 601623) gave normal results. In addition, all four individuals were susceptible to recurrent infections, which might be explained by the role of DEAF1 in interferon β gene transcription through interaction with interferon regulatory factor 3.[31] The behavioral abnormalities present in three of the four individuals consisted of autistic, hyperactive, and aggressive behavior with striking mood swings. Because DEAF1 has previously been linked to major depression and suicide through regulation of 5-hydroxytryptamine receptor 1A,[20–22] disturbance of the serotonin pathway might contribute to the phenotypes seen in the individuals reported here. Interestingly, in addition to the *DEAF1* mutation in the second individual, other candidate mutations were identified. The overlapping phenotype between this girl and the other individuals with mutations in *DEAF1* indicates that the mutation in *DEAF1* is the underlying cause.

We observed a high expression of *DEAF1* mRNA in the CNS in both humans and mice, as well as in zebrafish. This expression was observed in both fetal and adult human brain, whereas in zebrafish, *deaf1* expression was highest at earlier developmental stages. *Deaf1* has been previously reported to be widely expressed in mouse and rat tissues, as well as highly expression in the CNS.[6,32,33]

The expression of *DEAF1* at the high level found in the CNS might explain why mainly the nervous system is affected in these individuals.

We aimed to determine whether the different amino acid substitutions observed in the individuals with ID compromised normal functioning of DEAF1. All four de novo mutations altered the SAND domain, suggesting that these might result in inappropriate functioning of this domain. We tested the effect of the amino acid substitutions on three essential functions of the SAND domain, namely DNA binding, transcription regulation, and SAND-domain-mediated protein interactions. All four substitutions showed loss of transcriptional repression of the *DEAF1* promoter, indicating that all mutations identified in this study impair the normal function of *DEAF1* in transcriptional repression. In addition, three of the substitutions showed complete loss of DNA binding, and one showed greatly reduced DNA binding. Three of the four amino acid substitutions failed to activate the *Eif4g3* promoter, and two of them even resulted in a 10-fold suppression of transcription relative to basal expression levels. Three of the four substitutions also resulted in reduced interaction with XRCC6, indicating that for these substitutions, SAND domain function seems further compromised.

The impaired repression of the *DEAF1* promoter indicates that the de novo mutations as seen in these individuals could impair the normal function of DEAF1 by a loss-of-function effect. Contradictory to this hypothesis, however, is the observation that deletions including *DEAF1* have been reported for healthy controls[34] and that we identified a 1 bp insertion (chr11: g.674717del) leading to a frameshift (p.Leu441Trpfs*16) in *DEAF1* in a healthy individual (data not shown). Therefore, a more likely mechanism explaining the consequences of these *DEAF1* mutations might be a dominant-negative effect. Data that support this hypothesis are that all of the altered forms of DEAF1 were able to interact with a cytoplasmically localized DEAF1 and relocalize it to the nucleus and that two of the altered proteins produced dominant-negative activity in the transcriptional activation of *Eif4g3*. In previous large-scale exome sequencing studies, the importance of loss-of-function mutations was stressed,[35,36] but here we show the importance and clinical relevance of missense mutations most likely caused by effects different from loss of function.

Because the de novo mutations identified in individuals with ID most likely have dominant-negative activity, incapacitating both copies of *DEAF1*, we hypothesized that knockout of *Deaf1* in mice would result in behavior disorders. To test this hypothesis, we produced mice with a targeted disruption of *Deaf1*. Because our full knockout of *Deaf1* was embryonically lethal, we utilized a conditional knockout of *Deaf1* in the brain to perform studies on large enough cohorts of mice to obtain behavioral data. Partial survival of another *Deaf1*-knockout mouse was previously reported.[18] The increased lethality in our knockout mice could be due to strain differences, or the other mouse model could represent mice with partial retention of *Deaf1* function.

Mice with conditional homozygous knockout of *Deaf1* in neuronal tissues showed increased anxiety in the EPM and the open-field test. The increased anxiety behavior of the NKO mice might be relevant to the behavioral abnormalities observed in individuals with de novo *DEAF1* mutations. Fear-conditioning tests demonstrated a deficiency of NKO mice to freeze in response to foot shock, which additional testing indicated was unlikely to be due to diminished pain sensitivity, inferring that it might be related to an increased anxiety response of the mice. Compared to WT mice, both NKO and conditional heterozygous mice showed a lack of contextual memory in the fear-conditioning test after 24 hr. The memory deficits in the NKO mice might have relevance to higher-order cognitive deficiencies of individuals with ID. The observation that conditional heterozygous knockout mice also had memory deficits provides supporting evidence that the de novo *DEAF1* mutations observed in these heterozygous individuals might result in ID.

In conclusion, we show that de novo mutations affecting the SAND domain of the transcription factor DEAF1 cause a human phenotype characterized by ID with severe speech impairment and behavioral problems and provide various functional evidence that links dysregulation of *DEAF1* to the observed phenotype. Over the coming years, we expect many more mutations in *DEAF1* to be identified. Therefore, we established a website to collect detailed phenotypic data of individuals harboring *DEAF1* mutations not only to gain insight into the clinical spectrum that these mutations might cause but also to obtain fundamental understanding of the pathogenic mechanisms underlying *DEAF1*-related ID.

Supplemental Data

Supplemental Data include nine figures and five tables and can be found with this article online at http://dx.doi.org/10.1016/j.ajhg.2014.03.013.

Acknowledgments

We are grateful to the individuals involved and their parents for their participation. We would like to thank Hanka Venselaar for the in silico modeling of the *DEAF1* mutations. This work was supported by European Commission GENCODYS grant 241995 under the Seventh Framework Programme (to A.T.V.v.S. and B.B.A.d.V.), Netherlands Organisation for Health Research and Development grants 917-86-319 (to B.B.A.d.V.), 912-12-109 (to B.B.A.d.V. and J.A.V.), and 916-12-095 (to A.H.), NIH grants CA89438, CA137556, and HD060122 (to J.I.H. and M.W.C.), funds from the Southern Illinois University School of Medicine (to J.I.H. and M.W.C.), and funds from the Fraternal Order of Eagles in Carbondale (to J.I.H. and M.W.C.).

Received: January 29, 2014
Accepted: March 18, 2014
Published: April 10, 2014

Web Resources

The URLs for data presented herein are as follows:

Database of Genomic Variants, http://projects.tcag.ca/variation/
DEAF1 clinical website, http://www.deaf1gene.com
DECIPHER, http://decipher.sanger.ac.uk/
NHLBI Exome Sequencing Project (ESP) Exome Variant Server, http://evs.gs.washington.edu/
Online Mendelian Inheritance in Man (OMIM), http://www.omim.org
Project HOPE, http://www.cmbi.ru.nl/hope/home
RefSeq, http://www.ncbi.nlm.nih.gov/RefSeq
UCSC Genome Browser, http://genome-euro.ucsc.edu/cgi-bin/hgGateway?redirect=auto&source=genome.ucsc.edu

References

1. de Ligt, J., Willemsen, M.H., van Bon, B.W., Kleefstra, T., Yntema, H.G., Kroes, T., Vulto-van Silfhout, A.T., Koolen, D.A., de Vries, P., Gilissen, C., et al. (2012). Diagnostic exome sequencing in persons with severe intellectual disability. N. Engl. J. Med. *367*, 1921–1929.
2. Rauch, A., Wieczorek, D., Graf, E., Wieland, T., Endele, S., Schwarzmayr, T., Albrecht, B., Bartholdi, D., Beygo, J., Di Donato, N., et al. (2012). Range of genetic mutations associated with severe non-syndromic sporadic intellectual disability: an exome sequencing study. Lancet *380*, 1674–1682.
3. Veltman, J.A., and Brunner, H.G. (2012). De novo mutations in human genetic disease. Nat. Rev. Genet. *13*, 565–575.
4. Vissers, L.E., de Ligt, J., Gilissen, C., Janssen, I., Steehouwer, M., de Vries, P., van Lier, B., Arts, P., Wieskamp, N., del Rosario, M., et al. (2010). A de novo paradigm for mental retardation. Nat. Genet. *42*, 1109–1112.
5. Yang, Y., Muzny, D.M., Reid, J.G., Bainbridge, M.N., Willis, A., Ward, P.A., Braxton, A., Beuten, J., Xia, F., Niu, Z., et al. (2013). Clinical whole-exome sequencing for the diagnosis of mendelian disorders. N. Engl. J. Med. *369*, 1502–1511.
6. Huggenvik, J.I., Michelson, R.J., Collard, M.W., Ziemba, A.J., Gurley, P., and Mowen, K.A. (1998). Characterization of a nuclear deformed epidermal autoregulatory factor-1 (DEAF-1)-related (NUDR) transcriptional regulator protein. Mol. Endocrinol. *12*, 1619–1639.
7. Yip, L., Su, L., Sheng, D., Chang, P., Atkinson, M., Czesak, M., Albert, P.R., Collier, A.R., Turley, S.J., Fathman, C.G., and Creusot, R.J. (2009). Deaf1 isoforms control the expression of genes encoding peripheral tissue antigens in the pancreatic lymph nodes during type 1 diabetes. Nat. Immunol. *10*, 1026–1033.
8. Barker, H.E., Smyth, G.K., Wettenhall, J., Ward, T.A., Bath, M.L., Lindeman, G.J., and Visvader, J.E. (2008). Deaf-1 regulates epithelial cell proliferation and side-branching in the mammary gland. BMC Dev. Biol. *8*, 94.
9. Gross, C.T., and McGinnis, W. (1996). DEAF-1, a novel protein that binds an essential region in a Deformed response element. EMBO J. *15*, 1961–1970.
10. Yip, L., Creusot, R.J., Pager, C.T., Sarnow, P., and Fathman, C.G. (2013). Reduced DEAF1 function during type 1 diabetes inhibits translation in lymph node stromal cells by suppressing Eif4g3. J. Mol. Cell Biol. *5*, 99–110.
11. Bottomley, M.J., Collard, M.W., Huggenvik, J.I., Liu, Z., Gibson, T.J., and Sattler, M. (2001). The SAND domain structure defines a novel DNA-binding fold in transcriptional regulation. Nat. Struct. Biol. *8*, 626–633.
12. Michelson, R.J., Collard, M.W., Ziemba, A.J., Persinger, J., Bartholomew, B., and Huggenvik, J.I. (1999). Nuclear DEAF-1-related (NUDR) protein contains a novel DNA binding domain and represses transcription of the heterogeneous nuclear ribonucleoprotein A2/B1 promoter. J. Biol. Chem. *274*, 30510–30519.
13. Gibson, T.J., Ramu, C., Gemünd, C., and Aasland, R. (1998). The APECED polyglandular autoimmune syndrome protein, AIRE-1, contains the SAND domain and is probably a transcription factor. Trends Biochem. Sci. *23*, 242–244.
14. Jensik, P.J., Huggenvik, J.I., and Collard, M.W. (2012). Deformed epidermal autoregulatory factor-1 (DEAF1) interacts with the Ku70 subunit of the DNA-dependent protein kinase complex. PLoS ONE *7*, e33404.
15. Jensik, P.J., Huggenvik, J.I., and Collard, M.W. (2004). Identification of a nuclear export signal and protein interaction domains in deformed epidermal autoregulatory factor-1 (DEAF-1). J. Biol. Chem. *279*, 32692–32699.
16. Kateb, F., Perrin, H., Tripsianes, K., Zou, P., Spadaccini, R., Bottomley, M., Franzmann, T.M., Buchner, J., Ansieau, S., and Sattler, M. (2013). Structural and functional analysis of the DEAF-1 and BS69 MYND domains. PLoS ONE *8*, e54715.
17. Cubeddu, L., Joseph, S., Richard, D.J., and Matthews, J.M. (2012). Contribution of DEAF1 structural domains to the interaction with the breast cancer oncogene LMO4. PLoS ONE *7*, e39218.
18. Hahm, K., Sum, E.Y., Fujiwara, Y., Lindeman, G.J., Visvader, J.E., and Orkin, S.H. (2004). Defective neural tube closure and anteroposterior patterning in mice lacking the LIM protein LMO4 or its interacting partner Deaf-1. Mol. Cell. Biol. *24*, 2074–2082.
19. Veraksa, A., Kennison, J., and McGinnis, W. (2002). DEAF-1 function is essential for the early embryonic development of Drosophila. Genesis *33*, 67–76.
20. Czesak, M., Le François, B., Millar, A.M., Deria, M., Daigle, M., Visvader, J.E., Anisman, H., and Albert, P.R. (2012). Increased serotonin-1A (5-HT1A) autoreceptor expression and reduced raphe serotonin levels in deformed epidermal autoregulatory factor-1 (Deaf-1) gene knock-out mice. J. Biol. Chem. *287*, 6615–6627.
21. Lemonde, S., Turecki, G., Bakish, D., Du, L., Hrdina, P.D., Bown, C.D., Sequeira, A., Kushwaha, N., Morris, S.J., Basak, A., et al. (2003). Impaired repression at a 5-hydroxytryptamine 1A receptor gene polymorphism associated with major depression and suicide. J. Neurosci. *23*, 8788–8799.
22. Szewczyk, B., Albert, P.R., Burns, A.M., Czesak, M., Overholser, J.C., Jurjus, G.J., Meltzer, H.Y., Konick, L.C., Dieter, L., Herbst, N., et al. (2009). Gender-specific decrease in NUDR and 5-HT1A receptor proteins in the prefrontal cortex of subjects with major depressive disorder. Int. J. Neuropsychopharmacol. *12*, 155–168.
23. Manne, U., Gary, B.D., Oelschlager, D.K., Weiss, H.L., Frost, A.R., and Grizzle, W.E. (2001). Altered subcellular localization of suppressin, a novel inhibitor of cell-cycle entry, is an independent prognostic factor in colorectal adenocarcinomas. Clin. Cancer Res. *7*, 3495–3503.
24. O'Roak, B.J., Vives, L., Fu, W., Egertson, J.D., Stanaway, I.B., Phelps, I.G., Carvill, G., Kumar, A., Lee, C., Ankenman, K., et al. (2012). Multiplex targeted sequencing identifies recurrently mutated genes in autism spectrum disorders. Science *338*, 1619–1622.

25. Tronche, F., Kellendonk, C., Kretz, O., Gass, P., Anlag, K., Orban, P.C., Bock, R., Klein, R., and Schütz, G. (1999). Disruption of the glucocorticoid receptor gene in the nervous system results in reduced anxiety. Nat. Genet. *23*, 99–103.
26. Pollard, K.S., Hubisz, M.J., Rosenbloom, K.R., and Siepel, A. (2010). Detection of nonneutral substitution rates on mammalian phylogenies. Genome Res. *20*, 110–121.
27. Calabrese, R., Capriotti, E., Fariselli, P., Martelli, P.L., and Casadio, R. (2009). Functional annotations improve the predictive score of human disease-related mutations in proteins. Hum. Mutat. *30*, 1237–1244.
28. Li, B., Krishnan, V.G., Mort, M.E., Xin, F., Kamati, K.K., Cooper, D.N., Mooney, S.D., and Radivojac, P. (2009). Automated inference of molecular mechanisms of disease from amino acid substitutions. Bioinformatics *25*, 2744–2750.
29. Adzhubei, I.A., Schmidt, S., Peshkin, L., Ramensky, V.E., Gerasimova, A., Bork, P., Kondrashov, A.S., and Sunyaev, S.R. (2010). A method and server for predicting damaging missense mutations. Nat. Methods *7*, 248–249.
30. Venselaar, H., Te Beek, T.A., Kuipers, R.K., Hekkelman, M.L., and Vriend, G. (2010). Protein structure analysis of mutations causing inheritable diseases. An e-Science approach with life scientist friendly interfaces. BMC Bioinformatics *11*, 548.
31. Ordureau, A., Enesa, K., Nanda, S., Le Francois, B., Peggie, M., Prescott, A., Albert, P.R., and Cohen, P. (2013). DEAF1 is a Pellino1-interacting protein required for interferon production by Sendai virus and double-stranded RNA. J. Biol. Chem. *288*, 24569–24580.
32. LeBoeuf, R.D., Ban, E.M., Green, M.M., Stone, A.S., Propst, S.M., Blalock, J.E., and Tauber, J.D. (1998). Molecular cloning, sequence analysis, expression, and tissue distribution of suppressin, a novel suppressor of cell cycle entry. J. Biol. Chem. *273*, 361–368.
33. Zhang, J., Moseley, A., Jegga, A.G., Gupta, A., Witte, D.P., Sartor, M., Medvedovic, M., Williams, S.S., Ley-Ebert, C., Coolen, L.M., et al. (2004). Neural system-enriched gene expression: relationship to biological pathways and neurological diseases. Physiol. Genomics *18*, 167–183.
34. Iafrate, A.J., Feuk, L., Rivera, M.N., Listewnik, M.L., Donahoe, P.K., Qi, Y., Scherer, S.W., and Lee, C. (2004). Detection of large-scale variation in the human genome. Nat. Genet. *36*, 949–951.
35. O'Roak, B.J., Vives, L., Girirajan, S., Karakoc, E., Krumm, N., Coe, B.P., Levy, R., Ko, A., Lee, C., Smith, J.D., et al. (2012). Sporadic autism exomes reveal a highly interconnected protein network of de novo mutations. Nature *485*, 246–250.
36. Sanders, S.J., Murtha, M.T., Gupta, A.R., Murdoch, J.D., Raubeson, M.J., Willsey, A.J., Ercan-Sencicek, A.G., DiLullo, N.M., Parikshak, N.N., Stein, J.L., et al. (2012). De novo mutations revealed by whole-exome sequencing are strongly associated with autism. Nature *485*, 237–241.

The American Journal of Human Genetics, Volume *94*
Supplemental Data

Mutations Affecting the SAND Domain of DEAF1 Cause Intellectual Disability with Severe Speech Impairment and Behavioral Problems

Anneke T. Vulto-van Silfhout, Shivakumar Rajamanickam, Philip J. Jensik, Sarah Vergult, Nina de Rocker, Kathryn J. Newhall, Ramya Raghavan, Sara N. Reardon, Kelsey Jarrett, Tara McIntyre, Joseph Bulinski, Stacy L. Ownby, Jodi I. Huggenvik, G. Stanley McKnight, Gregory M. Rose, Xiang Cai, Andy Willaert, Christiane Zweier, Sabine Endele, Joep de Ligt, Bregje W.M. van Bon, Dorien Lugtenberg, Petra F. de Vries, Joris A. Veltman, Hans van Bokhoven, Han G. Brunner, Anita Rauch, Arjan P.M. de Brouwer, Gemma L. Carvill, Alexander Hoischen, Heather C. Mefford, Evan E. Eichler, Lisenka E.L.M. Vissers, Björn Menten, Michael W. Collard, and Bert B.A. de Vries

Figure S1 Recombinant proteins used in EMSA

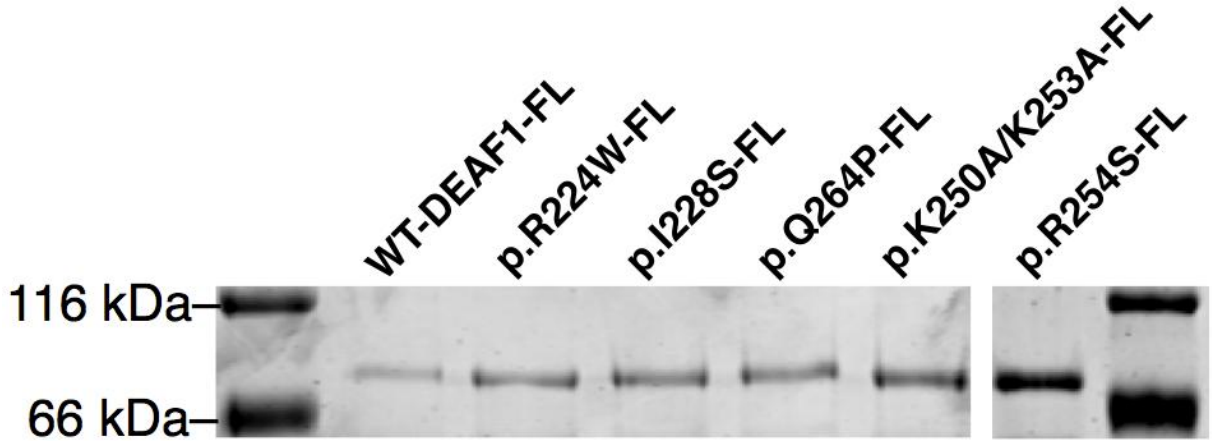

Recombinant WT and mutant DEAF1-FLAG were isolated from HEK 293 cells, separated by SDS-PAGE and stained with Coomassie blue. Left lane contains protein size standards; abbreviations of mutant proteins can be found in Figure 1 and 2 of the manuscript.

Figure S2 *DEAF1* expression in zebrafish and human tissues

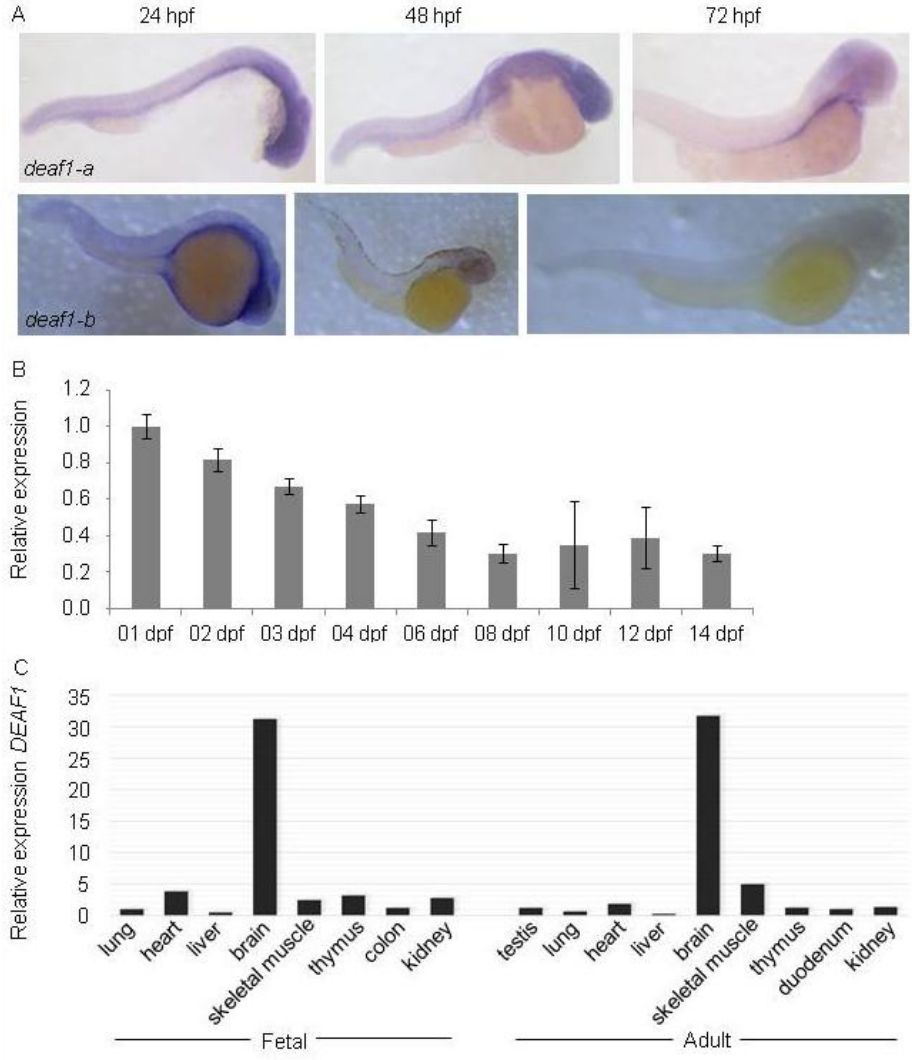

A. *Deaf1 in-situ* hybridization at various stages post fertilization in zebrafish embryos as previously described[2] with minor modifications. The primers used to design the hybridization probes are available in Table S1. *Deaf1* shows highest expression in brain and spinal cord. hpf = hours post fertilization.

B. Quantitation by qPCR of d*eaf1-a* expression at various post fertilization stages (8 and 16 hpf; 1-2-3-4-6-8-10-12-14 days post fertilization (dpf)) in zebrafish. Ten to twenty zebrafish embryos were dechorionated and collected per time point. The samples were homogenized in 200 µl trizol (QiaZol) and mixed with 40 µl chloroform. After centrifugation (4°C, 15 min, 12 rcf) the water phase was isolated, mixed with 100 µl isopropanol and incubated at room temperature (15 min). The precipitated RNA was

pelleted (4°C, 10 min, 12 rcf) and washed with 200 µl 75% ethanol (4°C, 5 min, 7.45 rcf). The pellet was air dried and subsequently resolved in 30 µl RNAse free water (60°C, 10 min). cDNA synthesis of these RNA samples was performed on 0.5 µg total RNA with the iScript kit (Bio-Rad Laboratories, Hercules, CA, USA) according to manufacturer's instructions. qPCR was performed with the Sso Advanced SYBR Green supermix (Bio-Rad Laboratories, Hercules, CA, USA) in a 5 µl reaction volume with 5 ng cDNA and 5 µM primers. Analysis was performed using the qbase^{+} software (http://www.biogazelle.com) and in-house validated reference genes (Vanhauwaert *et al.*, in preparation). Primers used for *deaf1-a* (zgc:194895) and *deaf1-b* (zgc:171506) are available in Table S1. *Deaf1-a* has highest expression at early developmental stages.

C. Expression of *DEAF1* by mRNA expression analysis in different human fetal and adult tissues. Relative expression levels are given as the fold change in comparison to the tissue with the lowest expression level (duodenum). Five microgram of total RNA from different human fetal (20-21 weeks) and adult tissues (Stratagene Europe, Amsterdam, the Netherlands) was reverse transcribed to cDNA using the iScript cDNA synthesis kit (BioRad Laboratories, Hercules, CA, USA) according to the manufacturer's protocol. SYBR green-based real-time quantitative PCR expression analysis was performed on a 7500 *Fast* Real-Time PCR System with the Power SYBR Green PCR Master Mix (Applied Biosystems, Foster City, CA, USA) according to the manufacturer´s instructions. Primers were designed by the primer3 program (http://frodo.wi.mit.edu/cgi-bin/primer3/primer3_www.cgi) and encompassed at least one exon-exon boundary. *GUSB* was used as a reference.[1] Primer sequences are provided in Table S1. Differences in *DEAF1* expression in the various tissues were calculated by the comparative Ct or $2^{\Delta\Delta Ct}$ method,[2] with the relative expression being determined by normalization of the *DEAF1* expressing tissues to the tissue with the lowest detectable expression of *DEAF1* set at 1.0.

Figure S3 Genomic structure of *Deaf1* targeted alleles in mice

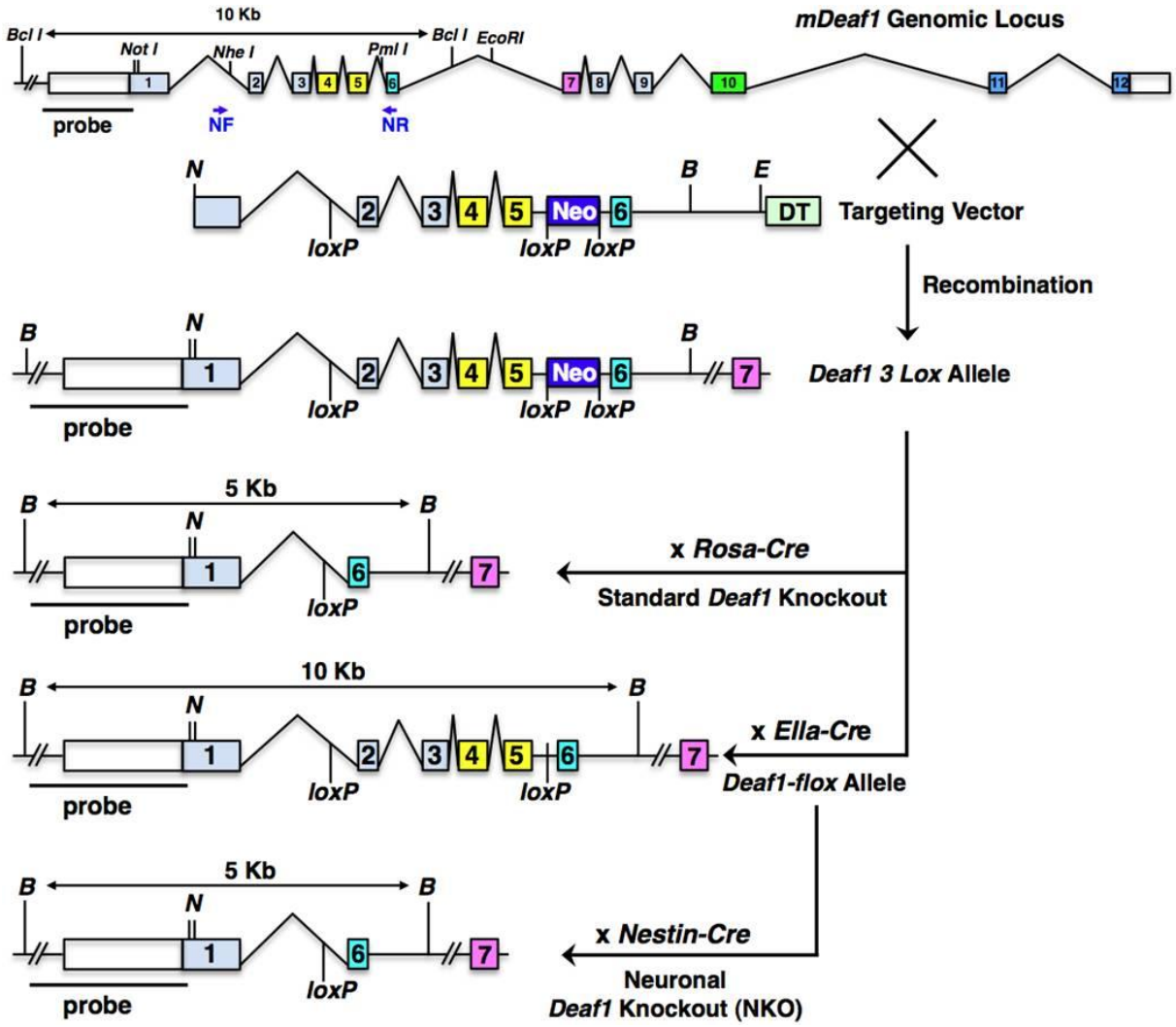

Schematic representations of the gene structures for the normal mouse *Deaf1* locus, the targeting vector, the *3loxP* allele, the standard *null* allele and the *Deaf1-floxed* allele and breeding schemes to produce them. *Deaf1* genomic clones were isolated from a mouse genomic 129/SvJ DNA lambda library (Stratagene #946313). The targeting vector contained a 10.1 Kb *Not*I/*EcoR*I fragment of *Deaf1* with a loxP sequence inserted into the *Nhe*I site, a *neomycin* gene cassette (Neo) flanked with loxP sites inserted into the *Pml*I site, and a *diptheria toxin* (DT) gene cassette inserted at the 3' end of the construct for positive selection of recombination in ES cells. The targeting construct was linearized with *Not*I and electroporated into 129J x 129J ES cells. Two independent ES cell clones were injected into C57BL/6 blastocysts to produce three chimeric mice that gave germ line transmission of the

"*3lox*" allele (transgenic mouse core at University of Washington, Seattle). For production of the null allele, mice with the *Deaf1 3lox* allele were bred to *Rosa-Cre* transgenic mice and offspriing with germline transmission of the null allele were outcrossed to C57BL/6 for greater than seven generations before genotype distribution of F2 mice and embryos were initially assessed (Table S2 and S4). Mice with a conditional *Deaf1* allele were produced using the "3loxP" approach of Xu et al.[3] Mice heterozygous for the *3lox* allele were backcrossed for nine generations onto a C57BL/6 strain background and were then bred to mice transgenic for *EIIa-Cre* gene (also on a C57BL/6 background). Partial recombination of loxP sites and removal of the neomycin cassette produced a *Deaf1* “2lox” or "floxed" allele with the genotype $Deaf1^{+/fl}$. The offspring were backcrossed again to C57BL/6 to assure congenic status, and subsequent $Deaf1^{+/fl}$ mice were maintained by breeding of $Deaf1^{+/fl}$ to each other. $Deaf1^{fl/fl}$ genomic structure was confirmed by genomic DNA sequencing at both loxP sites. In the upper diagram of the genomic locus functional domains are colored: the SAND domain is represented in yellow exons 4 and 5, a zinc-finger homology domain is shown in aqua exon 6, nuclear localization signal is in pink exon 7, nuclear export signal is in green exon 10, and the MYND domain is in blue exons 11 and 12. Restriction enzyme sites: *Bcl*I (B), *Not*I (N), *EcoR*I (E). When *loxP* is inserted into the *Nhe*I and *Pml*I sites of genomic DNA, the restriction sites are destroyed. NF and NR represent primers mDeaf1NP-F and mDeaf1NP-R (Table S1) in introns 1 and 5 that assay for the *null* allele following deletion of exons 2-5. "Probe" indicates a 1.2-Kb *Xho*I-*Apa*I DNA fragment used as a hybridization probe for Southern blot analysis of genomic DNA from F1 offspring (Figure S4A).

Figure S4 Confirmation of the *Deaf1* standard knockout mouse model

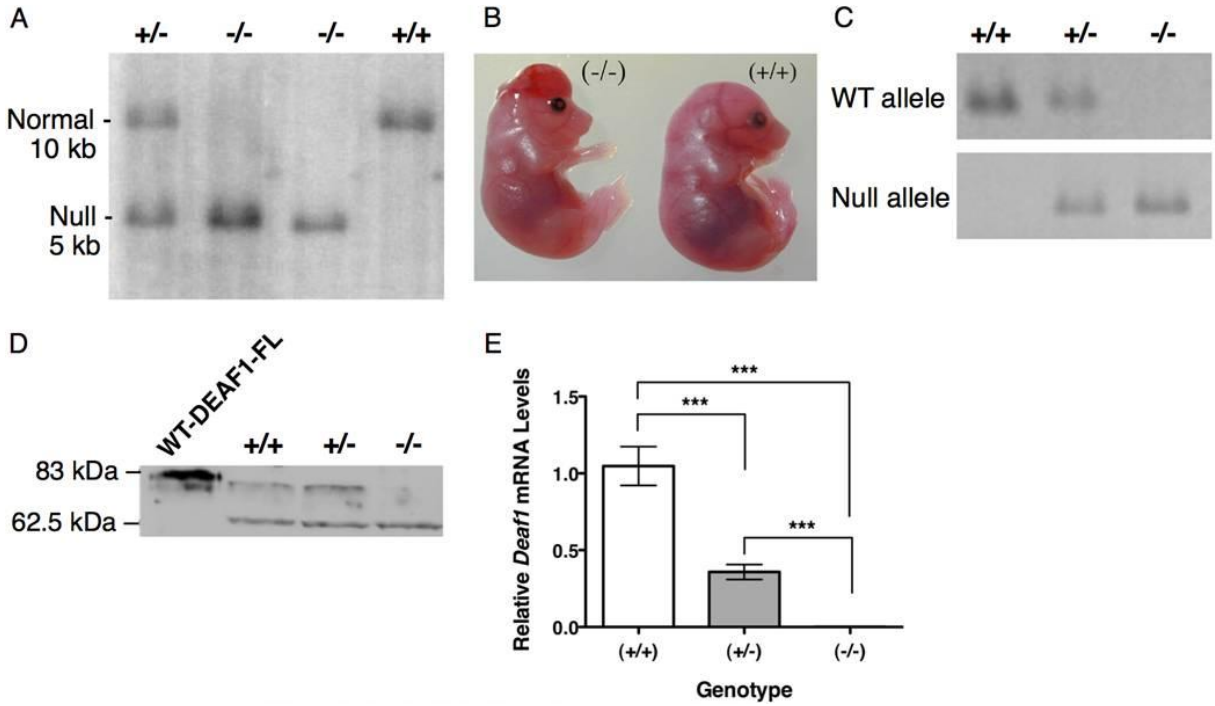

A. Southern blot analysis of *Bcl*I digested genomic DNA from F1 mouse embryo cells and hybridized to the radiolabeled DNA probe depicted in Figure S3.

B. Exencephaly phenotype observed in *Deaf1*$^{-/-}$ embryos.

C. PCR-based genotyping of genomic DNA from tail using primers mDlox5695F and mDlox5869R for assay of the WT allele, and primers mDeaf1NP-F and mDeaf1NP-R to assay the null allele (Table S1).

D. Loss of DEAF1 in *Deaf1*$^{-/-}$ embryos. Immunoblot blot of proteins in lysates from freshly isolated embryos and analyzed using a rabbit anti-DEAF1 antibody. Cell lysate from HEK 293T cells transfected with DEAF1-FLAG (DEAF1-FL) expression vector is used as a positive control in the far left lane. The 80 kDa DEAF1 protein is absent in *Deaf1*$^{-/-}$ embryos. The blot is representative of two independent experiments.

E. Loss of WT *Deaf1* mRNA in *Deaf1*$^{-/-}$ embryos. RNA was isolated from e18.5 F1 embryos: *Deaf1*$^{+/+}$ n=7, *Deaf1*$^{+/-}$ n=14, and *Deaf1*$^{-/-}$ n=9. Relative *Deaf1* mRNA levels were measured by qPCR using primers mDEAF696F and mDEAF769R that are specific for exon 5 and normalized to β-Actin (Table S1). Levels relative to *Deaf1*$^{+/+}$ were calculated by the $2^{-\Delta\Delta Ct}$

method[2] and reported as the mean ± SEM of three experiments, one-way ANOVA, Bonferroni post test, *** $p<0.001$

Figure S5 *Deaf1* mRNA expression in brain regions and liver of adult male control and NKO mice

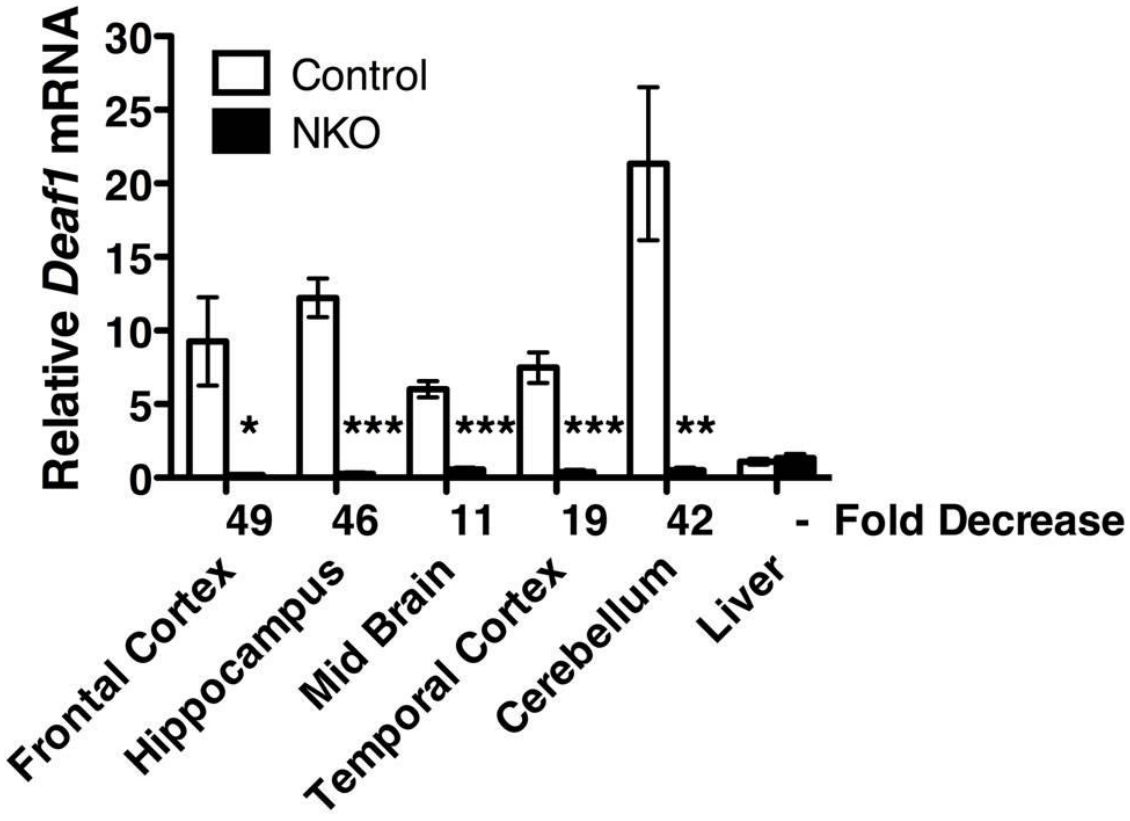

Relative *Deaf1* mRNA levels were measured by qPCR using primers mDEAF696F and mDEAF769R to exon 5 (Table S1) and normalized to β-Actin. RNA (3.5 µg) was primed with oligo(dT) and cDNA was generated using GoScript (Promega). *Quantitative PCR (qPCR)* was performed using a Bio-Rad CFX90 Real Time C1000 Thermal Cycler and Bio-Rad iQ SYBR Green Supermix. with the exon 5 specific primers. The Ct values obtained were normalized to mouse *β-actin* mRNA levels in each sample and relative gene expression in the samples were determined using the $2^{-\Delta\Delta Ct}$ method.[2] Levels relative to control liver were calculated by the $2^{-\Delta\Delta Ct}$ method[2] and are reported as the mean ± SEM. Control n=5, NKO n=5. Significant decreases were observed for NKO brain regions with no change in liver expression, two-way ANOVA with Bonferroni post test, * $p<0.05$, ** $p<0.01$, *** $p<0.001$.

Figure S6 Anxiety testing of mice with conditional heterozygous knockout of *Deaf1* in brain

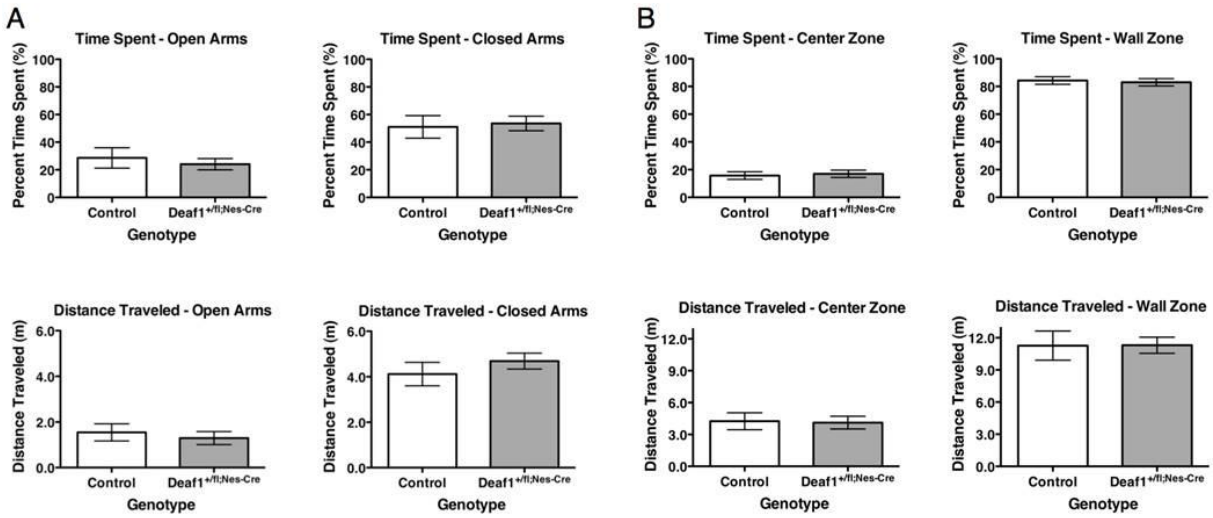

A. Anxiety testing using the elevated plus maze. Bars represent the mean ± SEM of time spent or distance traveled in open and closed arms. Control n=12, *Deaf1*$^{+/fl;Nes\text{-}Cre}$ n=13. No significant difference was observed between the two genotypes, unpaired two-tailed t-test.

B. Anxiety testing using the open field exploration test. Bars represent the mean ± SEM of time spent or distance traveled in center or wall zones. Control n=12, *Deaf1*$^{+/fl;Nes\text{-}Cre}$ n=15. No significant difference was observed between the two genotypes, unpaired two-tailed t-test.

Figure S7 Tests for depression-like behavior and mobility of mice with conditional knockout of *Deaf1* in brain

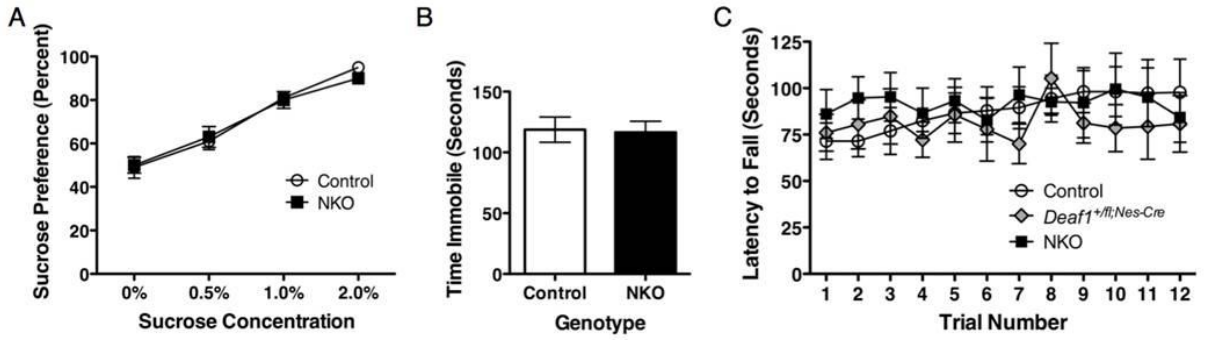

A. Sucrose preference, Control n=11, NKO n=11, mean ± SEM, No significant difference was observed between genotypes. The sucrose preference test was conducted similarly to that previously described.[4] Mice were individually housed during the testing period (48 hours) followed by group housing in between testing of different sucrose concentrations (24 hours). Food was provided *ad libitum*. During the testing period, the individually housed mice were given two bottles from which to drink, one containing plain tap water and the other containing sucrose with varying sucrose concentrations (0%, 0.5%, 1% and 2%) in tap water. The bottles were weighed at the beginning of the testing period (0 hour) and at the end (48 hours). The position of the bottles was switched at 24 hours to avoid possible side bias. Following the 48 hour testing period, mice were group housed along with their cage mates and provided with two bottles both containing plain tap water. After 24 hours of group housing, mice were again separated into individual cages and tested with a different concentration of sucrose. The process was repeated and after the final concentration, mice were permanently returned to group housing. The difference in weight in grams at 0 hour and 48 hours was calculated for the bottle containing plain tap water (ΔW) and the bottle containing tap water with sucrose (ΔS). Sucrose preference was calculated using the formula

$$\text{Sucrose preference } \% = \frac{\Delta S}{\Delta W + \Delta S} * 100$$

B. Forced swim, Control n=12, NKO n=12, mean ± SEM, No significant difference was observed between genotypes. Mice were individually placed in a clear plastic cylinder

(diameter 17 cm, height 24.5 cm) filled with water at room temperature (22-25°C) to a depth of 10 cm. Fresh water was used for each animal. The animal was placed in the cylinder for a total of six min, and behavior was recorded and analyzed using ANY-maze software for the last four min. Behavior was categorized as “swimming” or “immobility” (defined as the absence of active, escape-oriented behaviors such as swimming, jumping, rearing, sniffing or diving). A mouse was judged to be immobile when it stopped struggling and floated in an upright position, making only small movements to keep its head above water.

C. Rotarod, Control n=9, *Deaf1*$^{+/fl;Nes\text{-}Cre}$ n=9, NKO n=9, mean ± SEM, No significant difference was observed among genotypes. Mice were placed on a rotating-rod apparatus that accelerated linearly from 4 to 40 rpm over five minutes of the run. The mice were given three trials on each of four consecutive days with a one hour resting period between trials. The amount of time a mouse stayed on the rotating rod was plotted to a maximum time of five minutes, the duration of each trial. Two episodes of holding on instead of walking, as the rod rotated through 360 degrees was scored as a fall. The average for three trials for each day is plotted.

Figure S8 Morris water maze for learning and memory of mice with conditional knockout of *Deaf1* in brain

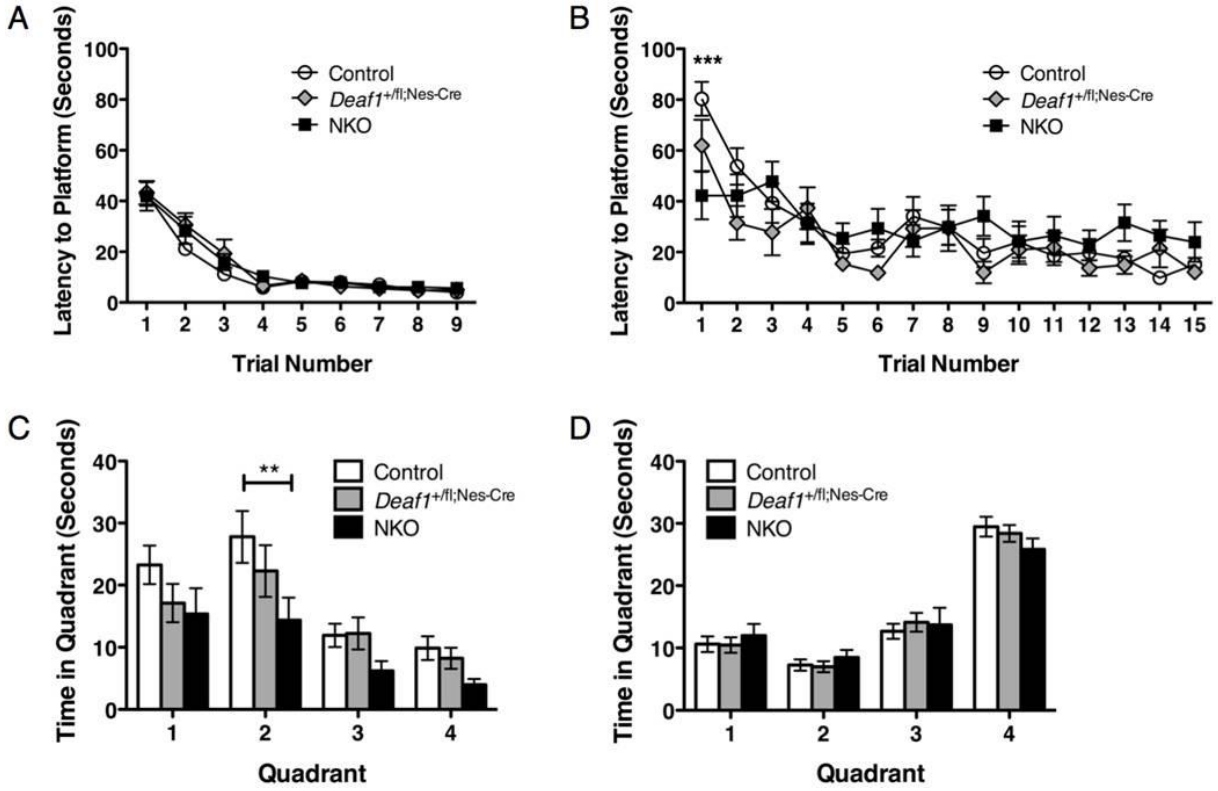

A. Morris Water Maze-Visible Platform, Control n=16, *Deaf1*$^{+/fl;Nes\text{-}Cre}$ n=12, NKO n=14, mean ± SEM, No significant difference was observed among genotypes.

B. Morris Water Maze-Hidden Platform, Control n=16, *Deaf1*$^{+/fl;Nes\text{-}Cre}$ n=12, NKO n=14, mean ± SEM, Two-way ANOVA, Bonferroni post test *** $p<0.001$ for Trial 1 between NKO and Control.

C. Morris Water Maze, Trial 1 of Quadrant Analysis of quadrant 4 with hidden platform (quadrant 2 with previously visible platform), Control n=16, *Deaf1*$^{+/fl;Nes\text{-}Cre}$ n=12, NKO n=14, mean ±SEM, Two-way ANOVA, Bonferroni post test ** $p<0.01$ between NKO and Control in quadrant 2.

D. Morris Water Maze, Quadrant Analysis, Probe Trial after 1 week, Control n=16, *Deaf1*$^{+/fl;Nes\text{-}Cre}$ n=12, NKO n=14, mean ± SEM, No significant difference was observed among genotypes.

Figure S9 Sensitivity to foot shock of NKO vs control

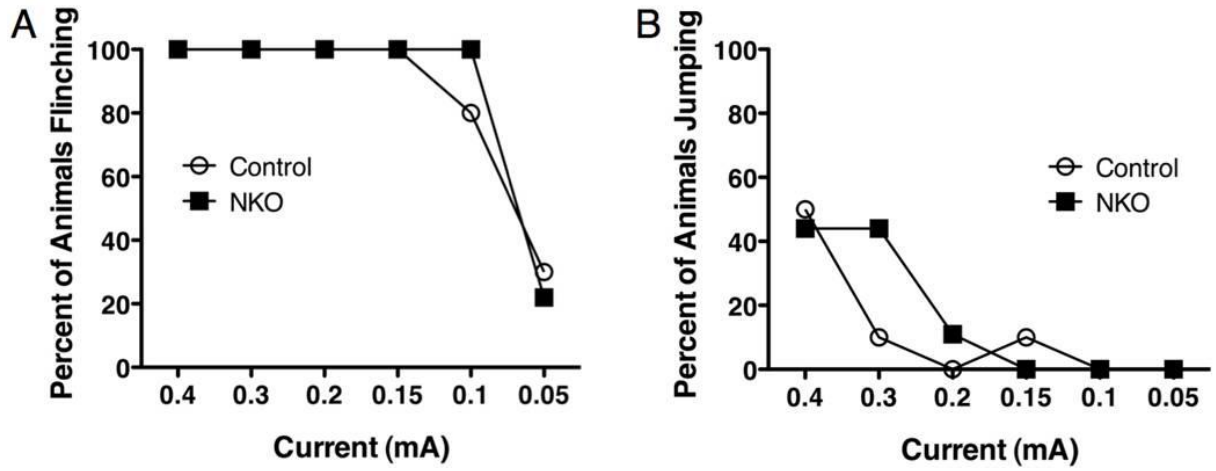

Foot shock sensitivity in mice was examined following fear conditioning testing. A jump is recorded if either all four limbs or the hind limbs alone leave the floor while the footshock is given. A flinch would be a noticeable response to the shock without a jump. Footshocks were given for one second each and mice were allowed to recover for 1 minute between shocks. Shock was applied in a descending order of intensity. The chamber was wiped with 70% ethanol and dried completely between mice. Mice of the indicated genotype were exposed to the indicated level of foot shock, starting from the highest to lowest mA value. Percent of animals flinching (A) and jumping (B) was recorded. Control n=10, NKO n=9. NKO mice have a similar response relative to control mice at the current used.

Table S1 Primers used in this study

Primer name	Sequence 5'->3'	Product size	Allele or Purpose
mDlox5695F	TAGAATTCGATCTATGGTGGGTGTG	174 bp (WT)	Wild Type
mDlox5869R	CATACATGGGGCACACCTAATTTAG	226 bp (+LoxP)	and LoxP
mDeaf1NP-F	TTGGGATTTGGGGTCAAGG	359 bp	Null
mDeaf1NP-R	AGTGGGTGTAGTGGTTAAGG		
C001	ACCAGCCACTATCAACTCG	199 bp	Cre
C002	TTACATTGGTCCAGCCACC		
mβactin1756	CCCTTTTTTTTGTCCCCCCAA	99 bp	qPCR of β-
mβactin1855R	AAGTCAGTGTACAGGCCAGC		actin mRNA
mDEAF696F	GTGTATCAAGCAGGGAGAAAAC	73 bp	qPCR of WT
mDEAF769R	CGGATGCTTCTCTTCCAGTC		*Deaf1* mRNA
Eif4g3-609F	aaagctagcCTGAATCCGCTCCATCCCTTCC	667 bp	Reporter
Eif4g3+58R	aaaaagcttCTCAACGAGCAGAGCATCCAAC		
N52-69F	AATTCTTCGGCTTCCCACTTCGGAATT	27 bp	dsDNA ligand
N52-69R	AATTCCGAAGTGGGAAGCCGAAGAATT		11 bp sp CG
S6conF	TTGAGTTCGGGTGTTCGGGCTCAA	24 bp	dsDNA ligand
S6conR	TTGAGCCCGAACACCCGAACTCAA		6 bp sp CG
Deaf1-aF	GGGTAAAGGTCGCTGTATC		ISH
Deaf1-aR	CTGCGTGTCCTCTTGAATG		*deaf1-a*
Deaf1-bF	TGGAAGGTGGACGAAGGAAA		ISH
Deaf1-bR	GGCAAACCTACCAGACTCCA		*deaf1-b*
Deaf1-aF	AATCTAAACCTCCTCCGGCC	154 bp	qPCR *deaf1-a*
Deaf1-aR	CTCTGACTGGCTTGTTTGGC		
Deaf1-bF	AGCATGGCATCTGACAGTGA	308 bp	qPCR *deaf1-b*
Deaf1-bR	CCCCACAAGTGACAGGAAGT		
DEAF1_ex4/5_F	TACGGTGCCGGAACATCAG	108 bp	qPCR of
DEAF1_ex4/5_R	CAAACTCGGTGGGACTGTACC		human tissues

Table S2 Distribution of *Deaf1* Genotypes of 133 F2 embryos from *Deaf1*$^{+/-}$ intercross after ≥7 generations of backcross on C57BL/6 strain

Genotype	Number of embryos (percent)
(+/+)	32 (24%)
(+/-)	68 (51%)
(-/-)	33 (25%)

Table S3 Distribution of exencephaly in 33 *Deaf1*$^{-/-}$ F2 embryos (e14.5 to e18.5) from *Deaf1*$^{+/-}$ intercross after ≥7 generations of backcross on C57BL/6 strain

Gender	Number analyzed	Number with exencephaly (percent)
Female	14	9 (64%)
Male	19	11 (58%)

Table S4 Survival to weaning of 131 F2 offspring from *Deaf1*$^{+/-}$ intercross after ≥8 generations of backcross on C57BL/6 strain

Genotype	Number of mice surviving to weaning (percent)
(+/+)	43 (31%)
(+/-)	96 (69%)
(-/-)	0 (0%)

Table S5 Birth statistics of 126 F2 offspring from *Deaf1*$^{+/-}$ intercross after ≥6 generations of backcross on BALB/c strain

Genotype	Number of dead neonates (with exencephaly)	Number of mice surviving to weaning (percent of 92 mice)
(+/+)	6 (0)	39 (43%)
(+/-)	14 (3)	50 (54%)
(-/-)	14 (4)	3 (3%)

Supplemental References

1. de Brouwer, A.P., van Bokhoven, H., and Kremer, H. (2006). Comparison of 12 reference genes for normalization of gene expression levels in Epstein-Barr virus-transformed lymphoblastoid cell lines and fibroblasts. Molecular diagnosis & therapy 10, 197-204.
2. Livak, K.J., and Schmittgen, T.D. (2001). Analysis of relative gene expression data using real-time quantitative PCR and the 2(-Delta Delta C(T)) Method. Methods 25, 402-408.
3. Xu, X., Li, C., Garrett-Beal, L., Larson, D., Wynshaw-Boris, A., and Deng, C.X. (2001). Direct removal in the mouse of a floxed neo gene from a three-loxP conditional knockout allele by two novel approaches. Genesis 30, 1-6.
4. Cai, X., Kallarackal, A.J., Kvarta, M.D., Goluskin, S., Gaylor, K., Bailey, A.M., Lee, H.K., Huganir, R.L., and Thompson, S.M. (2013). Local potentiation of excitatory synapses by serotonin and its alteration in rodent models of depression. Nature neuroscience 16, 464-472.